

LBL-8088
e.g.

THE OXIDIZING BEHAVIOR OF SOME
PLATINUM METAL FLUORIDES

Lionell Graham
(Ph. D. Thesis)

RECEIVED
LAWRENCE
BERKELEY LABORATORY

October 1978

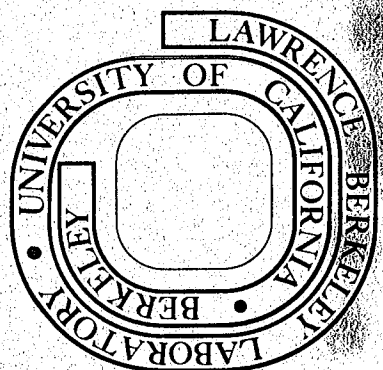
NOV 17 1978

LIBRARY AND
DOCUMENTS SECTION

Prepared for the U. S. Department of Energy
under Contract W-7405-ENG-48

TWO-WEEK LOAN COPY

*This is a Library Circulating Copy
which may be borrowed for two weeks.
For a personal retention copy, call
Tech. Info. Division, Ext. 6782*



LBL-8088
e.g.

LEGAL NOTICE

This report was prepared as an account of work sponsored by the United States Government. Neither the United States nor the Department of Energy, nor any of their employees, nor any of their contractors, subcontractors, or their employees, makes any warranty, express or implied, or assumes any legal liability or responsibility for the accuracy, completeness or usefulness of any information, apparatus, product or process disclosed, or represents that its use would not infringe privately owned rights.

THE OXIDIZING BEHAVIOR OF SOME
PLATINUM METAL FLUORIDES

Contents

Abstract	v
I. General Introduction	1
II. General Apparatus and Handling Techniques	2
A. Apparatus	2
1. General	2
2. The Cryogenic Technology, Inc., Model 21 Cryo-Cooler	3
3. Reactor for Gas-Gas Reaction Products	5
B. Reagents	5
1. Gases and Volatile Liquids	6
2. XeF ₂	7
3. Platinum Metal Reagents	7
(a) Metals	7
(b) Hexafluoro-Metals	7
(c) Other Platinum Metal Compounds	8
C. Instrumentation	10
1. Raman Spectroscopy	10
2. Infrared Spectroscopy	10
3. X-ray Powder Photography	11
4. Magnetic Susceptibility	11
5. Analysis	11
(a) Xenon	11
(b) Fluorine and Certain Platinum Metals by Pyrohydrolysis	12

Figures	13
References	17
III. Redox Reactions Related to the Xe/PtF ₆ Reaction	18
A. Introduction	18
B. Experimental	19
1. The Xe/PtF ₆ System	19
(a) Composition	19
(b) Magnetic Studies	20
(c) Structural Studies	21
2. Apparatus and Technique for the XeF ₂ /Platinum Fluoride and XeF ₂ /Palladium Fluoride Systems	22
3. The XeF ₂ /Platinum Fluoride System	22
(a) 2XeF ₂ ·PtF ₅	22
(b) XeF ₂ ·PtF ₅	23
(c) Pyrolysis of XeF ₂ ·PtF ₅ and the Formation of XeF ₄ and XeF ₂ ·2PtF ₄ (XePt ₂ F ₁₀)	24
4. The XeF ₂ /Palladium Fluoride System	24
(a) 4XeF ₂ ·PdF ₄ , 3XeF ₂ ·PdF ₄ , 2XeF ₂ ·PdF ₄	24
(b) XeF ₂ ·PdF ₄	25
(c) Pyrolysis of XeF ₂ ·PdF ₄ and the Formation of XeF ₂ ·2PdF ₄ (XePd ₂ F ₁₀)	25
(d) Pyrolysis of XeF ₂ ·2PdF ₄ with the Formation of XeF ₄ and Pd ₂ F ₆	25
C. Results and Discussion	26
Tables	34
Figures	41
References	48

IV. The Interaction of Chlorine with the Third-Series Transition Metal Hexafluorides and Related Studies . . .	50
A. Introduction	50
B. Experimental	54
1. The Cl_2/IrF_6 Studies	54
(a) The Stoichiometry of the Cl_2/IrF_6 Reaction Product	54
(b) Spectroscopic Studies of the Product of the Cl_2/IrF_6 Reaction	55
(c) Reactions of the Cl_2/IrF_6 Products	56
(i)NO, (ii) C_6F_6 in WF_6 , (iii) BrF_3 , (iv) ClO_2F , (v) IF_5	
2. The Cl_2/PtF_6 Studies	59
(a) The Stoichiometry of the Cl_2/PtF_6 Reaction Product	59
(b) Spectroscopic Studies of the Products of the Cl_2/PtF_6 Reaction	59
(c) Reactions of the Cl_2/PtF_6 Product(s)	60
(i)NO, (ii) Br_2	
3. Spectroscopic Studies of the Cl_2/OsF_6 Reaction	60
4. Spectroscopic Studies of the Cl_2/ReF_6 Reaction	61
5. Spectroscopic Studies of the Cl_2/WF_6 Reaction	61
6. Related Studies	62
(a) Reactions of $\text{Cl}_3^+\text{AsF}_6^-$	62
(i) C_6F_6 , (ii)ONF	
(b) Reaction of $\text{Cl}_2\text{F}^+\text{AsF}_6^-$ with ONF	62
(c) Attempted Reaction of ClF with Ir_4F_{20}	63

C. Results and Discussion	63
Tables	77
Figures	81
References	88
Acknowledgments	90

THE OXIDIZING BEHAVIOR OF SOME
PLATINUM METAL FLUORIDES

Lionell Graham

Inorganic Materials Research Division,
Lawrence Berkeley Laboratory and
Department of Chemistry
University of California
Berkeley, California 94720

ABSTRACT

The previously known compounds $\text{Xe}_2\text{F}_3^+\text{PtF}_6^-$, $\text{XeF}^+\text{PtF}_6^-$ and $\text{XeF}_2 \cdot 2\text{PtF}_4$ ($\text{XePt}_2\text{F}_{10}$) were prepared by the interaction of XeF_2 with PtF_4 . The new compounds $\text{XeF}_2 \cdot \text{PdF}_4$ and $\text{XeF}_2 \cdot 2\text{PdF}_4$ ($\text{XePd}_2\text{F}_{10}$) have been produced by interaction of XeF_2 with either PdF_4 or Pd_2F_6 . A weight loss-versus-time curve has indicated the presence of 4:1, 3:1 and 2:1 $\text{XeF}_2/\text{PdF}_4$ complexes. The thermal decomposition of XeFPtF_6 or $\text{XePd}_2\text{F}_{10}$ yields highly pure XeF_4 . Thus the interaction of XeF_2 with platinum fluorides (PtF_4 or PtF_5) or palladium fluorides (Pd_2F_6 or PdF_4) provides for the conversion of XeF_2 to XeF_4 . The compound $\text{XePd}_2\text{F}_{10}$ is a close structural relative of $\text{XePt}_2\text{F}_{10}$, and spectroscopic evidence suggests that both are salts of XeF^+ and a polymeric $(\text{M}_2\text{F}_9)_x^-$ ion.

A $\text{Xe}:\text{PtF}_6$ material of approximately 1:1 stoichiometry has been prepared and compared with XePdF_6 ($\text{XeF}_2 \cdot \text{PdF}_4$).

The interaction of chlorine with the third-series transition metal hexafluorides has been investigated. Gravimetric and tensimetric evidence indicate that the initial product of the Cl_2 plus IrF_6 reaction is a solid of composition Cl_2IrF_6 . Vibrational spectroscopic and other evidence indicates that this solid yields a sequence of products, of

which $\text{Cl}_3^+\text{IrF}_6^-$, $\text{Cl}_3^+\text{Ir}_2\text{F}_{11}^-$ and Ir_4F_{20} have been identified, the last being the ultimate solid product of the room temperature decomposition of the adduct. A new chlorine fluoride generated in the room temperature decomposition of Cl_2IrF_6 has been tentatively formulated as Cl_3F from infrared evidence.

I. GENERAL INTRODUCTION

The studies described in this thesis are divided into two topics: (1) a study of xenon complexes involving platinum and palladium fluorides and (2) a study of the oxidation of molecular chlorine by third-series transition metal hexafluorides. The investigation of the interaction of xenon with PtF_6 is closely related to the studies of the oxidation of Cl_2 by transition metal hexafluorides and links the two topics.

The techniques and specially constructed apparatus common to the two topics are described in Chapter II. This chapter also contains brief descriptions of the instrumentation used in the experimental work. Techniques and apparatus developed for one particular project are described in the appropriate section.

Chapter III is concerned with topic (1) and is broadly concerned with the characterization of the solid products formed from the interaction of xenon and platinum hexafluoride and with the thermal decomposition of those solids. The products of the interaction of xenon difluoride with PtF_4 , PdF_4 and Pd_2F_6 became an important component of this investigation.

Chapter IV deals with the long-standing problem of whether or not the Cl_2^+ radical cation is capable of existence in the crystalline state. The investigation of this problem, via the Cl_2 plus third-series transition metal hexafluoride interactions, has yielded some unexpected findings.

II. GENERAL APPARATUS AND HANDLING TECHNIQUES

A. Apparatus

1. General

The ease of hydrolysis and powerfully oxidizing character of most of the compounds used or prepared in this work necessitated the employment of rigorously dry conditions for their handling. These properties also required careful selection of container materials.

A Vacuum Atmospheres Corporation Dri-lab (North Hollywood, California) provided the dry inert atmosphere (nitrogen) used for manipulation of the various solids and liquids encountered in this work. Both oxygen and water were minimized in the Dri-lab by two circulating drying trains which were regenerated on a regular schedule.

Volatile compounds were manipulated using a vacuum line constructed from Autoclave Engineering 30VM6071 Monel valves (rated to 30,000 Psi) and appropriate connectors. Vacuum was provided by three separate pumps: (1) a small mechanical pump joined to the line via a soda lime tower for disposal of volatile corrosive fluorides and fluorine; (2) a large mechanical pump used for high-speed pumping capability when corrosive materials were absent; and (3) for high-vacuum capability, a two-inch Consolidated Vacuum Corporation silicone-oil diffusion pump coupled to a high-vacuum manifold.

Low pressures (< 1 mm) were measured using a Hastings thermocouple gauge. Pressures in the 0-1500 torr Hg range and the 0-500 psia range were determined with Helicoid gauges supplied by Acco Helicoid Gage (Bridgeport, Connecticut), constructed from Monel. These Helicoid

gauges were constructed especially for fluorine or oxygen service.

Each newly assembled or reassembled apparatus was leak-tested using a Consolidated Electrodynamics Corporation quadrupole mass spectrometer helium leak detector.

High pressure and/or high temperature reactions were carried out in bombs fabricated from Monel metal, tested to 500 atmospheres of gaseous fluorine at 600°C.

2. The Cryogenic Technology, Inc., Model 21 Cryo-Cooler (Waltham, Massachusetts)

This device consisted of a cold-head, a compressor unit with an absorber, and interconnecting piping. Helium was used as the refrigerant. It was capable of producing cryo-tip temperatures down to 10°K.

A hydrogen vapor pressure gauge (16°-26°K), in addition to a chromel versus gold and 0.07% Fe thermocouple, was used for temperature measurement.

The temperature was controlled in three ways: (1) by off-setting the capacity of the refrigerator with an electrical ~~"button-type"~~ resistance heater which was embedded in the underside of the cryo-tip; (2) by using an external infrared lamp focused on the sample; and (3) by switching off the refrigerator. The last provided for particularly slow warming.

The vacuum shroud, developed for this work, was, for operational convenience, divided into two parts, as shown in Figure II-1. One section, which was joined directly to the cryo-cooler, remained permanently attached to the device. It consisted of a cylinder provided with two entry ports, one for an eight-pin electrical feed-through, the

other for a vacuum gate valve. The eight-pin feedthrough allowed for operation of electrical heating and for thermocouple leads. A flange on the cylinder provided for attachment of the second part of the shroud. This part contained four window apertures: two, for infrared spectroscopy, were set opposite to one another and on an axis at right angles to the cylindrical shroud axis; the remaining two facilitated Raman spectroscopy, the smaller aperture, for the incident laser beam, being at right angles to the shroud axis and to the axis of the infrared window apertures. The larger Raman window aperture axis coincided approximately with the axis of the shroud cylinder.

The cryo-tip, shown in Figure II-2, was fashioned from a silver block. A honeycomb of holes was drilled through the block (in preference to one large opening) to ensure good thermal contact between the block and the infrared window attached to it. This window, upon which volatile samples were deposited, coincided with the axis of the two infrared window apertures previously described. One corner of the block, situated just below the incident laser light aperture, was shaved to an angle of 20° . This highly polished surface allowed for scattering of the incident laser beam in the direction of the larger Raman window aperture. The disc-shaped base of the block provided for connection to the second stage of the cold station.

Two 1/8-inch diameter lengths of copper tubing were passed through the wall of the second part of the shroud and were sealed in place with silver solder. These provided for direction of the flow of gaseous reactants onto the cryo-tip. By situating the ends of these tubes approximately one inch from the edge common to the silver chloride

window and the surface for Raman scattering, adequate opportunity for gas-gas interaction was provided for.

Gas flow was regulated with the aid of two stainless steel Nupro SS-4MA (manufactured by Nupro Company, Cleveland, Ohio) fine metering valves. Each of these valves gave access to the component of the vacuum system which was used solely for one of the reactant gases.

The entire assembly, including vacuum line, mechanical pump, cold chamber, compressor unit, etc., was mounted on a mobile cart. The cold chamber, resting on a laboratory jack, could be raised or lowered to allow for either Raman or infrared spectroscopy.

3. Reactor for Gas-Gas Reaction Products

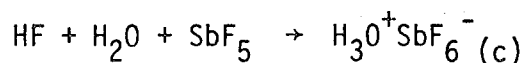
The gram quantity preparations of gas-gas interaction products were carried out using a reactor of the type shown in Figure II-3. It consisted of a Kel-F tube swaged to a Monel assembly. The assembly provided for introduction of the reactant gases through separate 1/8-inch diameter copper tubes which terminated within the Kel-F collector. A 1/4-inch diameter tube let into the head of the assembly provided for connection to the high vacuum system. The lower region of the Kel-F tube (\sim two inches) was kept at -196°C during a reaction. This provided for rapid quenching of the product.

B. Reagents

Many reagents were used as supplied. Some were subjected to extensive purification and others had to be prepared by following or adapting procedures described in the literature.

1. Gases and Volatile Liquids

NO, BrF₃, Cl₂, F₂, IF₅ and HF were supplied by the Matheson Company (East Rutherford, New Jersey). NO was purified by fractional distillation at =160°C. Its purity was checked by infrared spectroscopy. BrF₃, contaminated with bromine and possibly bromine monofluoride, was purified by fluorination at room temperature. Cl₂ (research grade) was used directly from the cylinder. Its purity was checked using infrared and Raman spectroscopy. F₂ was freed of hydrogen fluoride by passing the impure fluorine through a copper U-tube cooled to liquid oxygen temperature. IF₅, contaminated with iodine, was purified by fluorination at room temperature. HF was dried by distilling it on to antimony pentafluoride contained in a Kel-F vessel. Small quantities of water were removed according to the following reaction, as given by Christie:¹



Anhydrous HF was distilled from the mixture at 0°C.

Xenon was used as supplied by Airco Industrial Gases (Santa Clara, California). No detectable impurities were observed for solid xenon using infrared and Raman spectroscopy.

C₆F₆ was used directly as supplied by P.C.R., Inc. (Gainesville, Florida).

ClO₂F was obtained as an impurity in ClF supplied by the Matheson Company. The more volatile ClF was removed by vacuum distillation at -110°C. The purity of ClO₂F was checked by infrared spectroscopy.²

ONF was prepared following the method of Ratcliffe and Shreeve.³

ClF was prepared by mixing equimolar quantities of Cl_2 and F_2 at approximately 90°C . Its purity was checked using infrared spectroscopy.⁴

2. XeF₂

Xenon difluoride was prepared by mixing equimolar quantities of xenon and fluorine in a five-liter pyrex vessel, followed by irradiation with UV light, according to the method of Streng and Streng⁵ and Holloway,⁶ as given by Williamson.⁷ It was checked for purity by infrared spectroscopy on the gas (2.5 mm at 25°C) and Raman spectroscopy on the solid.

3. Platinum Metal Reagents

(a) Metals

Platinum wire (0.040 inch), iridium, osmium and rhenium sponge (all specified to be at least 99.9% pure) were supplied by Engelhard Industries (Union, New Jersey).

(b) Hexafluoro-metals

Hexafluorides of the transition metals were prepared by standard procedures, as indicated below. Each was characterized using both infrared and Raman spectroscopy. The Raman spectra of the solid binary fluorides are shown in Figure II-4.

The following list gives the reference to the procedure followed in the preparation of each material:

<u>Material</u>	<u>Literature Reference</u>
Platinum hexafluoride	Wienstock, Malm and Weaver ⁸
Iridium hexafluoride	Ruff and Fischer ⁹
Osmium hexafluoride	Wienstock and Malm ¹⁰
Rhenium hexafluoride	Malm and Selig ¹¹

Tungsten hexafluoride was used as supplied by Matheson Gas Products.

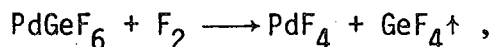
(c) Other Platinum Metal Compounds

Palladium dibromide was obtained by dissolving palladium sponge in aqueous hydrobromic acid-bromine mixture. The mixture was heated with an infrared lamp and bromine was added from time to time until all the palladium metal had dissolved. The resultant solution was passed through a sintered glass filter and was then evaporated to dryness under an infrared lamp. The purple-to-black solid was dried further by holding it under a vacuum of approximately 10^{-6} torr overnight.

PdGeF₆ was prepared by dissolving a 1:1 molar mixture of PdBr₂ and germanium tetrabromide (used as obtained from Ventron Alfa Products, Cerritos, California) in bromine trifluoride. The PdBr₂:GeBr₄ mixture was contained in a Kel-F tube and bromine trifluoride was distilled onto it at -196°C. The mixture was warmed slowly. (Caution: The initial stage of the reaction is extremely vigorous; the liquid N₂ coolant should be kept close at hand.) The beginning of the reaction was signalled by bromine evolution and was moderated (when necessary) by judicious cooling with liquid N₂. As the reaction proceeded, the evolved bromine served as a diluent and the vigor of the reaction moderated. When obvious signs of reaction had ceased, the mixture was warmed to approximately 70°C to ensure completion of the reaction; the volatiles were removed under vacuum. The brown, solid residue was heated to 200°C in a vacuum to ensure complete removal of bromine trifluoride.

Palladium tetrafluoride was prepared by the fluorination of

PdGeF_6 . Fluorination of lower palladium fluorides was used by Bartlett and Rao¹² to prepare the first samples of PdF_4 , but their product was always contaminated by PdPdF_6 . Crystalline PdPdF_6 is highly resistant to oxidation. The fluorination of PdGeF_6 :



overcame this difficulty. PdGeF_6 , prepared as described above, was heated to 280°C, with fluorine (at 780 psi at 20°C), for approximately 58 hours in a heavy-walled Monel copper gasketed bomb, provided with a Monel valve (see General Apparatus). The resultant PdF_4 ¹³, which was a pink powder, showed no X-ray powder lines of Pd_2F_6 . The Raman spectrum of PdF_4 is as shown in Figure III-3, that of PdPdF_6 is included since it is a common impurity in PdF_4 and is even produced by pyrolysis, with intense laser sources, in the Raman experiment.

Platinum tetrabromide was prepared by first dissolving platinum metal in aqua regia. A large excess of HBr was then added to the resultant solution and it was evaporated to dryness over an open flame in the fume hood. The dark red solid residue was dried further by placing it in an oven for two days at a temperature of 70°C.

Platinum tetrafluoride was either prepared by pyrolysis of $\text{XePt}_2\text{F}_{10}$ at 430°C or according to the following method which is an adaptation of that given by Sharpe.¹⁴ The action of bromine trifluoride on platinum tetrabromide gave a red solution from which the 2:1 adduct $(\text{BrF}_3)\text{PtF}_4$, was isolated. Thermal decomposition of this adduct at 180°C gave platinum tetrafluoride contaminated with a small amount of bromine trifluoride. Remaining BrF_3 was removed by fluorination at 200°-250°C.

Palladium trifluoride was prepared according to the method of Sharpe¹⁴ or by the pyrolysis of $\text{XePd}_2\text{F}_{10}$ under vacuum at 300°C.

C. Instrumentation

1. Raman Spectroscopy

Raman spectra were obtained using two different instruments, both of which employed a double monochromator and a detection system that utilized photon counting. Initially, spectra were recorded using a Spex 1401 double monochromator coupled to an on-line computer which allowed data to be collected, stored, normalized and plotted. Subsequent spectra were obtained using a Ramanor HG, 2S spectrometer. A variety of excitation wave lengths (blue 488.0 nm, green 514.5 nm, and red 647.1 nm) were available from the Spectra Physics Model 165 Krypton and Coherent Radiation Model CR-2 Argon ion lasers. For those materials which were thermally stable at room temperature, samples were loaded into quartz capillaries (1.0 to 1.5 mm o.d.) as used in X-ray diffraction (see below), in the Dri-lab. They were sealed temporarily with a plug of Kel-F grease, and the tube was drawn down in a small flame outside the box. Thermally unstable or volatile compounds were either deposited onto the cryo-tip of the cryo-cooler or prepared in situ in small quartz vessels described under IV.B below. Samples were cooled by flowing dry N_2 which was itself cooled by passage through a 3/8-inch diameter copper coil immersed in liquid N_2 (-196°C).

2. Infrared Spectroscopy

Infrared spectra were obtained on a Perkin-Elmer Model 337 Grating Spectrophotometer over the range 4,000-400 cm^{-1} . The spectra of

gases were obtained using a 10 cm path length Monel cell fitted with silver chloride windows. These windows were cut from 1 mm sheet obtained from Harshaw Chemical Company, Cleveland, Ohio. Spectra of solids were obtained from dusted samples of the solids pressed between silver chloride sheets (1 mm) in a Kel-F holder. It was necessary to deposit thermally unstable samples onto the silver chloride window of the cryo-cooler described under II.A.

3. X-Ray Powder Photography

X-ray powder photographs were obtained using a General Electric Precision Powder Camera of 45 cm circumference (Straumanis loading) with Cu- α radiation and a graphite monochromator. Finely powdered samples were loaded into 0.3-0.5 mm thin-walled quartz capillaries (made in Western Germany and obtained from Charles Supper Company, Inc., Natick, Massachusetts) in an identical manner to that described under Raman spectroscopy. X-ray films were measured on a Norelco film-measuring device.

4. Magnetic Susceptibility

Magnetic susceptibility measurements were made using a Princeton Applied Research vibrating sample magnetometer in the temperature range 3.5-100°K. Solid samples, 0.1-0.18g, were loaded into specially fabricated Kel-F tubes. A tight-fitting plug was pressed down firmly on the sample to ensure tight packing.

5. Analysis

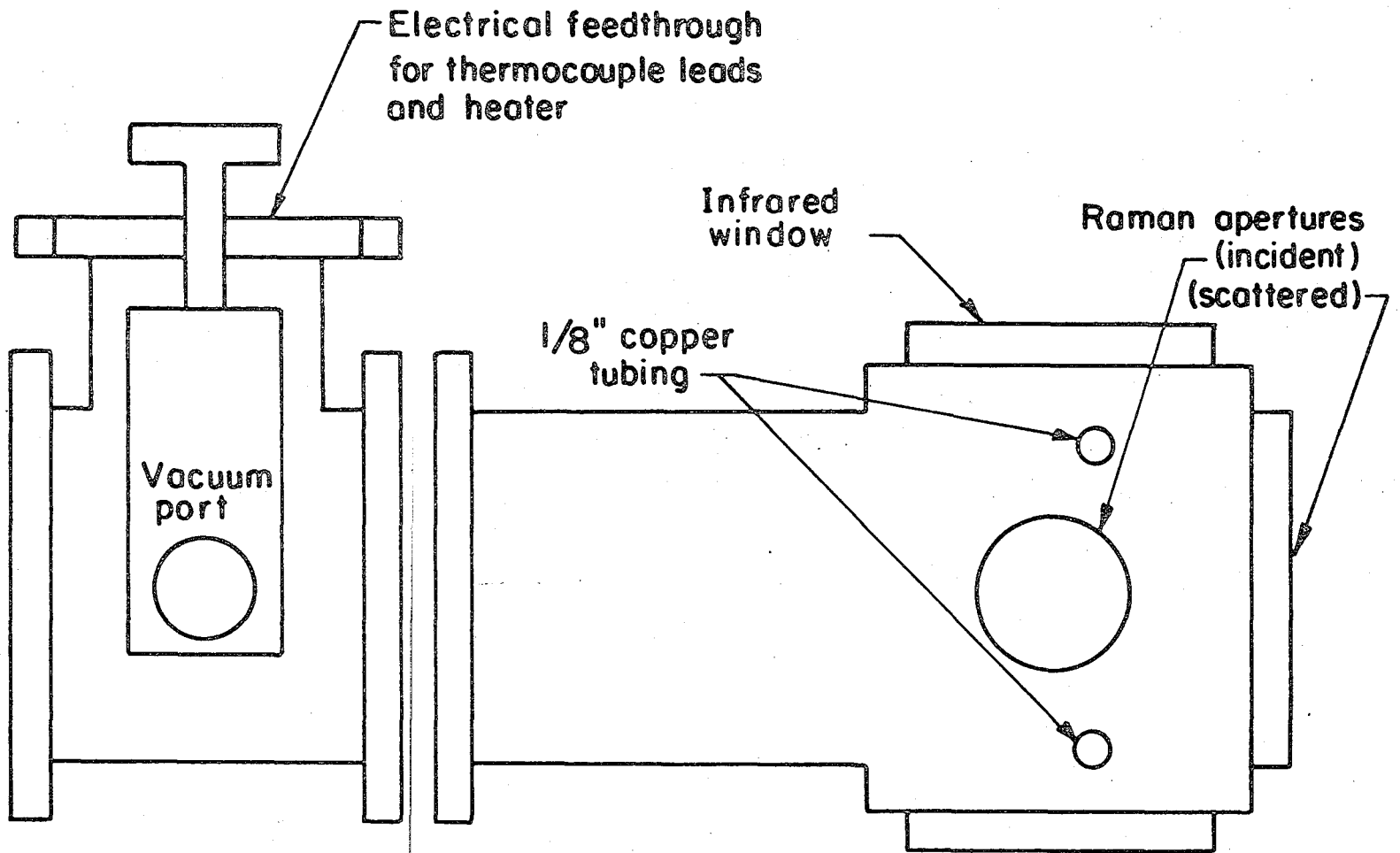
(a) Xenon

Xenon was determined using a Dumas nitrometer. Samples were loaded into preweighed, thin-walled pyrex capillaries in the same

manner as described under Raman spectroscopy. The capillaries were weighed prior to loading and the loaded tube and the drawn-off part were also weighed to provide the sample weight. The loaded tube was placed in the chamber of the nitrometer which was raised to 800°C. The evolved gas was collected over 50% KOH solution previously saturated with xenon.

(b) Fluorine and Certain Platinum Metals by Pyrohydrolysis

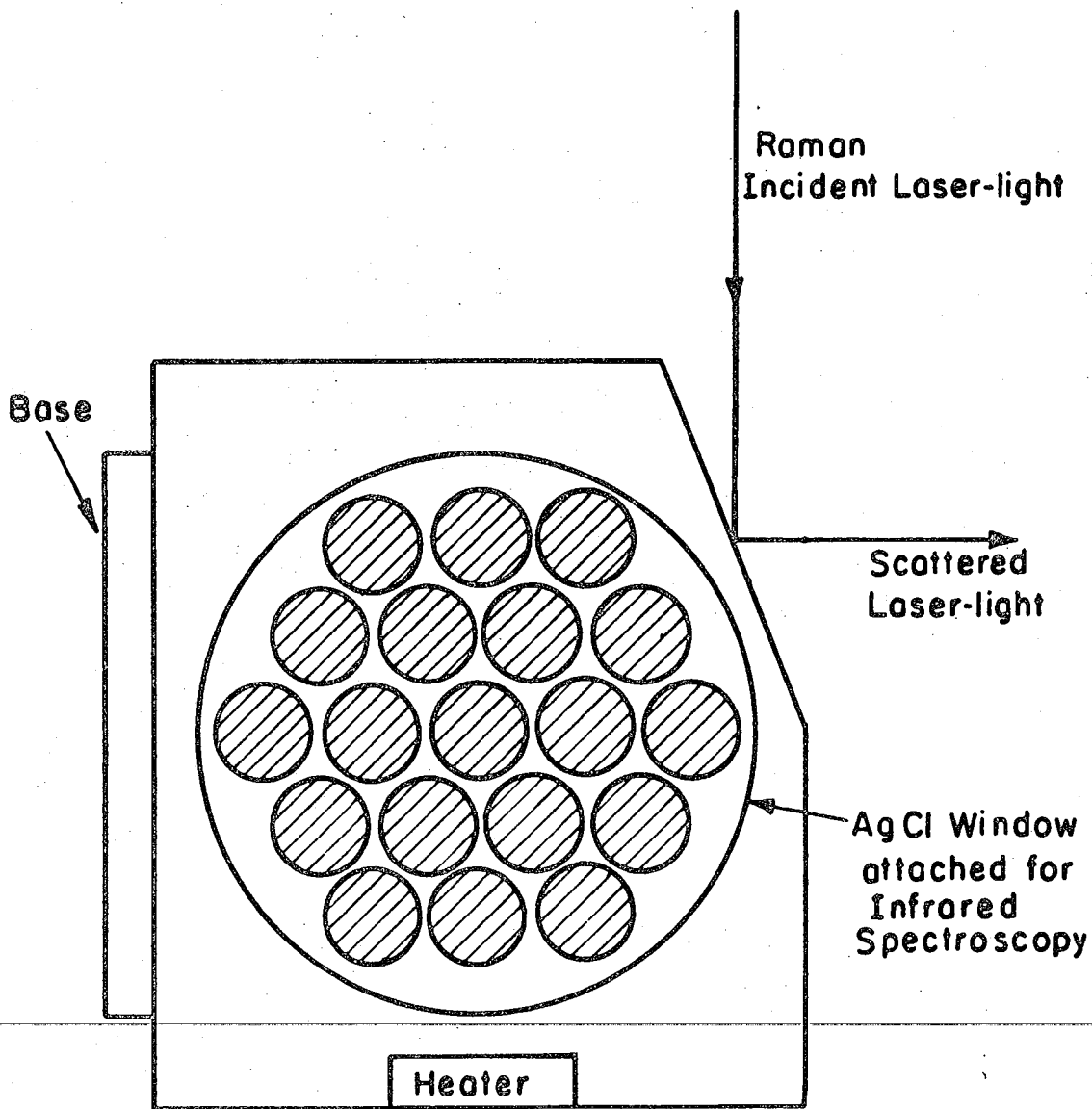
The platinum group metals and fluorine were estimated using the pyrohydrolysis analytical technique.^{15,16,17} The solid sample, 0.2-0.3g, was placed in the Dri-lab into a preweighed platinum boat and the boat was reweighed. The boat was contained, for weighing purposes, in a glass tube with teflon end caps. The loaded boat was transferred to the pyrohydrolysis tube by removing the teflon caps and pushing the boat as quickly as possible into the pyrohydrolysis tube. Water-laden nitrogen was passed over the sample, initially at room temperature. ~~The emerging nitrogen stream was bubbled through water collecting any~~ hydrogen fluoride produced in the hydrolysis. The temperature of the furnace, surrounding the pyrohydrolysis tube, was increased until steam passed over the sample at approximately 300°C. The fluoride ion concentration was estimated by titration with 0.10 N NaOH, using phenolphthalein as an indicator. Fluoride in the solution was also determined gravimetrically by precipitation as lead chlorofluoride. In the cases of platinum and palladium fluorides, the residue in the boat provided for determination of the metal content. The residue was heated to 400°C in a stream of hydrogen and thus gave the pure metal.



-13-

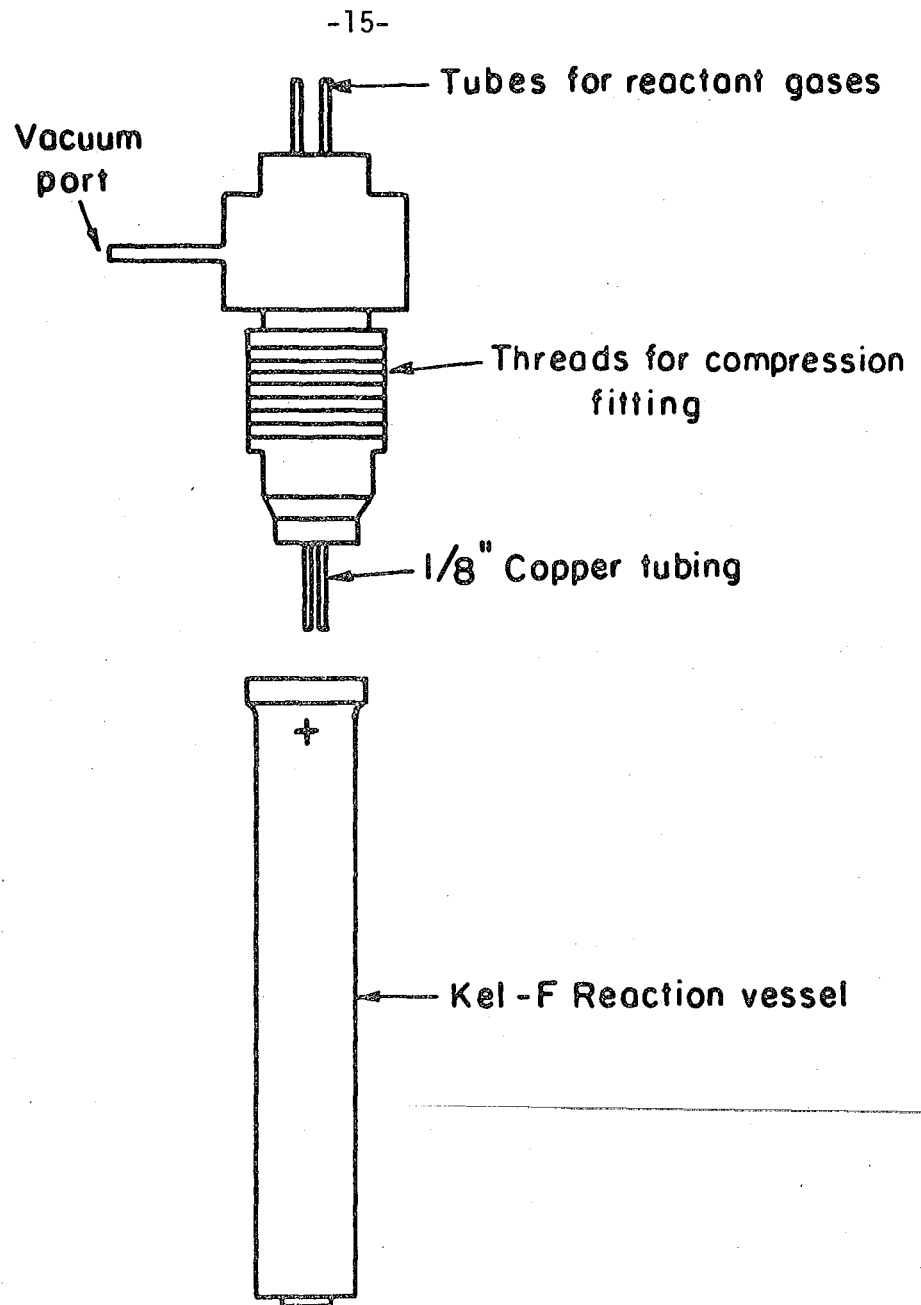
Figure I-1. Two-piece vacuum shroud for cryo-tip.

XBL787-5346



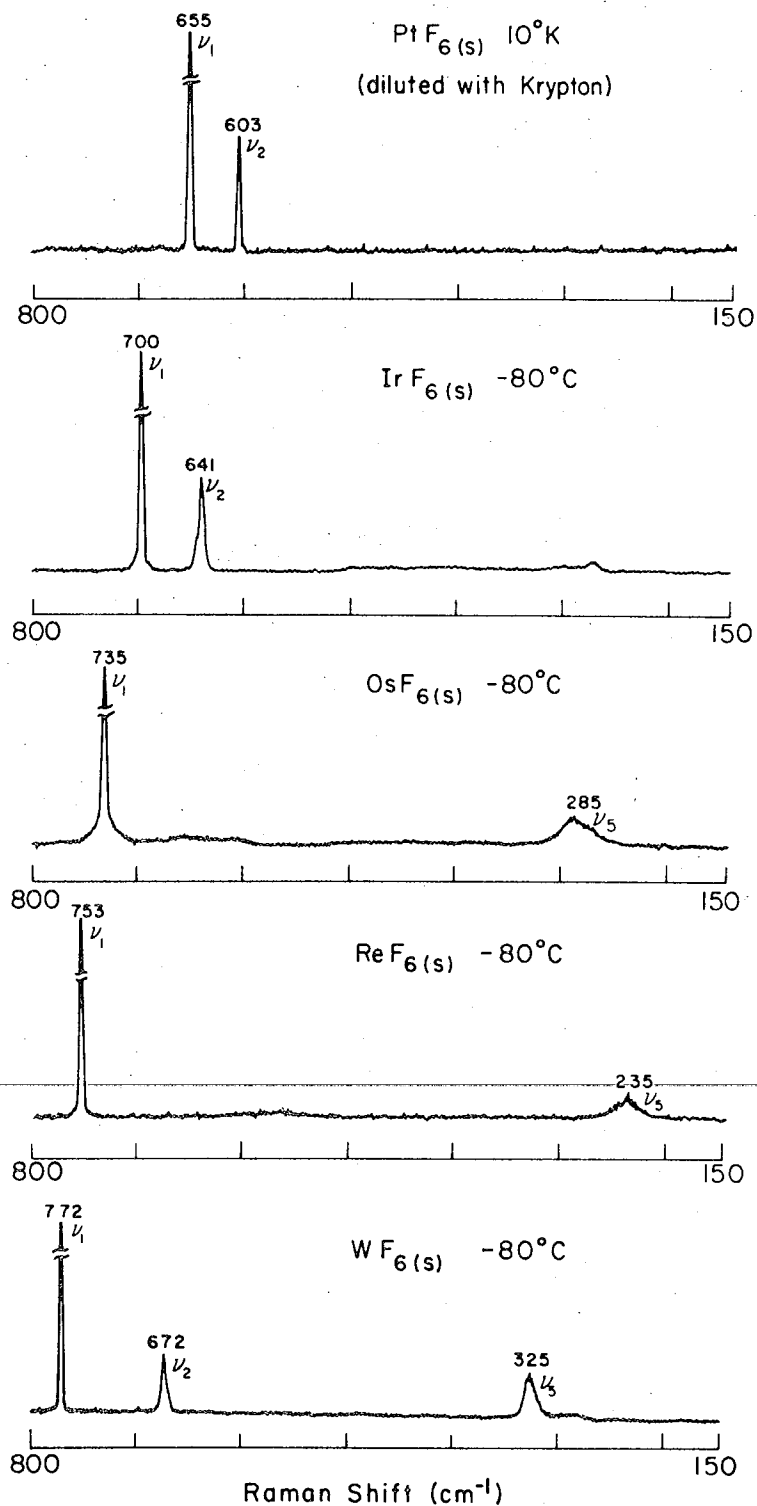
XBL787-5347

Figure I-2. Silver cryo-tip for infrared and Raman spectroscopy.



XBL 737-5348

Figure I-3. Kel-F reactor with Monel attachment.



XBL 787-5355

Figure I4. Raman spectra of the third-series transition metal hexafluorides.

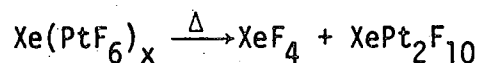
REFERENCES

1. K.O. Christie, C.J. Schack and R.D. Wilson, *Inorg. Chem.* 14, 2224 (1975).
2. A.J. Arvia and P.J. Aymonino, *Spectrochimica Acta* 20, 1763 (1964).
3. C.T. Ratcliffe and J.M. Shreeve, *Inorg. Synthe.* 11, 194 (1968).
4. E.A. Jones, T.F. Parkinson and T.G. Burke, *J. Chem. Phys.* 18, 235 (1950).
5. L.V. Streng and A.G. Streng, *Inorg. Chem.* 4, 1370 (1965).
6. J.H. Holloway, *Chem. Comm.* 1, 22 (1966).
7. S.M. Williamson, *Inorg. Synthe.* 11, 147 (1968).
8. B. Wienstock, J.G. Malm and E.E. Weaver, *J. Amer. Chem. Soc.* 83, 4310 (1961).
9. O. Ruff and J. Fischer, *Z. Anorg. Allgem. Chem.* 179, 161 (1929).
10. B. Wienstock and J.G. Malm, *J. Amer. Chem. Soc.* 80, 4466 (1958).
11. J.G. Malm and H. Selig, *J. Inorg. and Nucl. Chem.* 20, 189 (1961).
12. N. Bartlett and P.R. Rao, *Proc. Chem. Soc.*, 343 (1964).
13. P.R. Rao, A. Tressand and N. Bartlett, *J. Inorg. and Nucl. Chem. Supplement*, 23 (1976) and A.F. Wright, B.E.F. Fender, N. Bartlett and K. Leary, *Inorg. Chem.* 17, 748 (1978).
14. A.G. Sharpe. *J. Chem. Soc.*, 3444 (1950).
15. D.H. Lohmann, Ph.D. Thesis, University of British Columbia (1961).
16. G.A. Welch and N. Parker, U.K.A.E.A. unclassified report, WSL-R-36 (1959).
17. J.D. Rushmere and H. Messon, U.K.A.E.A. unclassified report, SC5-R-392 ARDC/P-84 (1959).

III. REDOX REACTIONS RELATED TO THE Xe/PtF₆ REACTION*

A. Introduction

Bartlett and Jha¹ showed in 1962 that the oxidation of xenon by platinum hexafluoride yielded a product with a stoichiometry that varied between XePtF₆ and Xe(PtF₆)₂. Chemical and physical evidence indicated that the oxidation state of the platinum in Xe(PtF₆)_x was +5. The pyrolysis of Xe(PtF₆)_x, at 165°C produced xenon tetrafluoride as the volatile product (xenon itself was not sought) according to:



The residue was a red solid of composition XePt₂F₁₀, the diamagnetism of which suggested a Pt(IV) compound. There was, however, no proof that this material was even a single phase.

The above observations suggested that Pt(V) fluorides had (at least under certain circumstances) the capability to oxidize Xe(I) or Xe(II) to Xe(IV).

Bartlett et al.² had shown from earlier studies that xenon difluoride formed 2:1, 1:1 and 1:2 complexes with platinum pentafluoride, which had been characterized, respectively, as Xe₂F₃⁺PtF₆⁻, XeF⁺PtF₆⁻ and XeF⁺Pt₂F₁₁⁻. The diamagnetism of XePt₂F₁₀ obtained¹ by Bartlett and Jha indicated that it was probably a Pt(IV) complex, but the stoichiometry rested upon sparse analytical data. A prime goal was therefore to confirm the existence of a 1:2 XeF₂:PtF₄ complex. Whether

*The substance of this chapter appeared in the J. Fluorine Chem. 7, 301 (1976).

or not complexes of PtF_4 richer in XeF_2 could be prepared was also of interest and the 1:1 compound particularly so, since it offered the prospect of a valence isomer of $\text{Xe}^+\text{PtF}_6^-$.¹

Since Pd(IV) fluorocomplexes are usually structurally similar³ to their Pt(IV) relatives, it appeared probable that XeF_2 with PdF_4 might yield the palladium analogue of $\text{XePt}_2\text{F}_{10}$ and of any other $\text{PtF}_4/\text{XeF}_2$ complex which might occur. Studies of the interactions of XeF_2 both with PtF_4 and with PdF_4 were therefore undertaken. These studies were subsequently broadened to include the interaction of the mixed-valence palladium fluoride, Pd_2F_6 .

B. Experimental

1. The Xenon-Platinum Hexafluoride System

(a) Composition

Initial experiments were designed to prepare the $\text{Xe}:\text{PtF}_6$ product of approximately 1:1 stoichiometry. Platinum hexafluoride, diluted with sulfur hexafluoride (1:6), was bled slowly through a length of 1/8 in. copper tubing into a Kel-F vessel (see Figure II-3) while simultaneously flowing xenon into the same vessel through a separate length of tubing but at a faster flow rate. The flow rate of the reactant gases was regulated by passing them each through Monel Nupro SS-4MA metering valves. These valves were coupled to the 1/8 in. lengths of copper tubing via a 1/4-1/8 in. reducing union. The lower portion of the approximately 6 in. Kel-F reactor was maintained at -196°C . Thus the product formed by the gas-gas interaction was quickly quenched, along with excess xenon and sulfur hexafluoride diluent.

This technique allowed for preparation of the approximately 1:1 product in gram amounts. The resultant, finely divided, mustard-yellow solid was retained on removal of sulfur hexafluoride and xenon at -80°C . Further warming to room temperature produced no other volatiles. Several samples of the product were prepared and analyzed for xenon and/or platinum:

Preparation	Xe(%)	Pt(%)
1	27.5	45.0
2	26.6	44.6
3	26.0	--
4	25.2	--
5	25.5	--
6	33.2	--
XePtF ₆ requires	29.8	44.3
Xe(PtF ₆) ₂ requires	17.5	52.1

(b) Magnetic Studies

The room temperature magnetic susceptibility of $\sim 1:1$

Xe:PtF₆ was measured by the Guoy technique. Low temperature measurements ($\sim 4^{\circ}\text{C}$ to 100°K) were carried out using the Vibrating Sample Magnetometer. The samples were loaded as described under II.C. Measurements of several analysed samples were made and are tabulated below. The χ_g vs. T plot for the two of the samples (1 and 3) are compared with that of XeF⁺PtF₆⁻ (see Figure III-7).

Preparation Number (see Table above)

1. $T^{\circ}\text{K}$	3.6	14.0	25.6	46.0	85.7	296
$10^5 \chi_g(\text{cgs})$	3.79	1.86	1.36	1.07	0.908	1.66
3. $T^{\circ}\text{K}$	3.6	22.1	36.4	55.6	65.4	99.3
$10^5 \chi_g(\text{cgs})$	5.97	1.43	1.00	0.772	0.727	0.568
5. $T^{\circ}\text{K}$	4.0	10.9	30.7	51.6	78.9	112.5
$10^5 \chi_g(\text{cgs})$	5.56	2.38	0.863	0.590	0.431	0.318

It is possible that the susceptibility value from the room temperature measurement does reflect the uncoupled moments for Xe^+ and PtF_6^- , each of which is paramagnetic, and the lower susceptibilities observed at low temperatures are due to an antiferromagnetic coupling of the Xe^+ and PtF_6^- magnets. Clearly, however, a susceptibility temperature study over the whole range should be carried out to confirm this coupling conjecture.

(c) Structural Studies

Further studies were carried out using the cryo-cooler described under II.A. The neat gas phase interaction of xenon (excess) and platinum hexafluoride once again produced a mustard-yellow solid. The product, however, was deposited onto a AgCl window, cooled to 10°K , suitable for infrared spectroscopy. The product buildup was signaled by an infrared absorption centered at 650cm^{-1} (see Figure III-1). The intensity of the band increased as long as the two gases were deposited. The absorption frequency appears in the region indicative of the ν_3 mode of the hexafluoroplatinate (V) ion. Numerous attempts were made to obtain X-ray powder patterns of the approximately 1:1 material but

it always proved to be amorphous.

2. Apparatus and Techniques for the XeF₂/Platinum Fluoride and XeF₂/Palladium Fluoride Systems

All of the XeF₂/platinum fluoride and the XeF₂/palladium fluoride systems were studied using the same reactor type. This was a 2 3/4 in. length of 3/8 in. Monel tube made by boring out rod to provide a wall and bottom thickness of 1/16 in. This tube was fitted with a 3/8-1/4 in. Swagelock reducing union. The tube was, depending upon the application, either closed with a 1/4 in. Swagelock cap or by a brass IKS4 Whitey valve (Kel-F tipped stem).

The thermal decomposition studies were initially carried out by following weight loss as functions of time and temperature of the sample when under vacuum. When the lowest temperature for rapid weight-loss had been established, the standard procedure was to hold the sample at this temperature until constant weight was attained. The volatiles were trapped at -196°C and were subsequently examined by gas infrared spectroscopy. The residual solids in the Monel tubes were examined by X-ray powder photography, Raman and infrared spectroscopy and were also subjected to magnetic susceptibility measurements.

The detailed conditions and findings are given in Table III-1.

3. The XeF₂ Platinum Fluoride System

(a) 2XeF₂·PtF₅

Typically, platinum tetrafluoride (0.2-0.4g) was weighed by difference into a Monel tube similar to that described above. An excess of xenon difluoride (1-2g) was then added to the tube. The tube was closed with a 1/4 in. Swagelock cap, weighed, and then buried in sand

in an electrically heated furnace. The temperature of the furnace was increased to 140-150°C and held constant for ~ 48 hours. Subsequently, the cap was replaced with a valve in the Dri-lab and XeF₂ and remaining xenon were removed under vacuum. The resultant bright yellow solid, Xe₂F₃⁺PtF₆⁻,² remained in the Monel reaction vessel.

Properties of 2XeF₂·PtF₅

The Raman spectrum of Xe₂F₃⁺PtF₆⁻ is shown in Figure III-2. The bright yellow salt decomposed in the blue (488.0 nm) laser light and the spectrum shown was obtained using the red excitation (647.1 nm) with moderate cooling of the sample. X-ray powder photographs (see Table III-2) showed the solid to be Xe₂F₃⁺PtF₆⁻, isomorphous with Xe₂F₃⁺MF₆⁻ (M=Ru, Ir) all previously prepared by Bartlett and his co-workers.²

(b) XeF₂·PtF₅

Pyrolysis of Xe₂F₃⁺PtF₆⁻ (0.6-1.0g) at 70°C for approximately 16 hours produced the 1:1 Pt(V) salt XeF⁺PtF₆⁻. The volatiles removed at this temperature were examined by infrared spectroscopy and proved to be pure XeF₂.

Properties of XeF₂·PtF₅

The Raman spectrum of XeF⁺PtF₆⁻ is shown in Figure III-2. The reported melting point is 82-83°C. X-ray photographs showed the solid to be identical to XeF⁺PtF₆⁻ prepared previously from PtF₅ and XeF₂.² The 1:1 XeF₂:PtF₅ salt has a yellow color but not nearly as intense as the 2:1 Pt(V) salt. Pyrolysis using the blue excitation (488.0 nm) was again observed.

(c) Pyrolysis of $\text{XeF}_2 \cdot \text{PtF}_5$ and the Formation of XeF_4 and $\text{XeF}_2 \cdot 2\text{PtF}_4$ ($\text{XePt}_2\text{F}_{10}$)

The thermal decomposition of the 1:1 salt, $\text{XeF}^+\text{PtF}_6^-$, under vacuum for several hours at 140°C produced a brown compound of composition $\text{XeF}_2:2\text{PtF}_4$ ($\text{XePt}_2\text{F}_{10}$). Infrared monitoring of the volatiles removed at this temperature showed pure xenon tetrafluoride.

Properties of $\text{XePt}_2\text{F}_{10}$

The Raman spectrum of $\text{XePt}_2\text{F}_{10}$ is shown in Figure III-3. The brown colored solid is diamagnetic as expected for the composition $\text{XeF}_2 \cdot 2\text{PtF}_4$, since both XeF_2 and PtF_4 have no unpaired electrons. $\text{XePt}_2\text{F}_{10}$ is thermally stable up to approximately 400°C under vacuum, where it then gives up XeF_2 . The resultant light brown solid was characterized as platinum tetrafluoride by its X-ray powder pattern and by its Raman spectrum given in Figure III-3.

4. The XeF_2 /Palladium Fluoride System

(a) $4\text{XeF}_2 \cdot \text{PdF}_4$, $3\text{XeF}_2 \cdot \text{PdF}_4$, $2\text{XeF}_2 \cdot \text{PdF}_4$

The XeF_2 /palladium fluoride system was studied in a manner similar to the XeF_2 /platinum fluoride system. An excess of XeF_2 (1-2g) was combined with either Pd_2F_6 or PdF_4 (0.2-0.6g) contained in a capped Monel tube. The vessel was then heated in a furnace at 140 - 150°C for ~ 48 hours. Subsequently, the volatiles and residual solids were examined.

In the first experiments, weight loss versus time curves, at 0°C , were plotted (care being taken that a constant sample temperature was maintained while volatiles were being removed). These studies gave evidence (clear changes in the slope of the curve) for the 4:1, 3:1 and

2:1 $\text{XeF}_2 \cdot \text{PdF}_4$ complexes.

(b) $\text{XeF}_2 \cdot \text{PdF}_4$

Exposure of the 4:1, 3:1 and 2:1 $\text{XeF}_2 \cdot \text{PdF}_4$ complexes to a dynamic vacuum, at $\sim 20^\circ\text{C}$, to constant weight produced a material of composition $\text{XeF}_2 \cdot \text{PdF}_4$. Throughout the fall of the compounds richer in XeF_2 , to this more stable material, the only volatile proved (by infrared spectroscopy) to be XeF_2 .

Properties of $\text{XeF}_2 \cdot \text{PdF}_4$

The Raman and infrared bands for $\text{XeF}_2 \cdot \text{PdF}_4$ are listed in Table III-3. The yellow solid is diamagnetic indicating Xe(II) and Pd(IV). The solid was amorphous to X-rays, not even broad lines being discernible in the X-ray powder photographs.

(c) Pyrolysis of $\text{XeF}_2 \cdot \text{PdF}_4$ and the Formation of $\text{XeF}_2 \cdot 2\text{PdF}_4$
 $(\text{XePd}_2\text{F}_{10})$

Decomposition of the 1:1 $\text{XeF}_2 \cdot \text{PdF}_4$ complex at $140\text{--}150^\circ\text{C}$ in a vacuum for several hours produced XeF_2 as the sole volatile and a light brown resultant solid of composition $\text{XePd}_2\text{F}_{10}$. X-ray powder photographs of this solid were strikingly similar to that of the analogous Pt(IV) salt, $\text{XePt}_2\text{F}_{10}$. (See Table III-4.)

Properties of $\text{XePd}_2\text{F}_{10}$

The Raman spectrum of $\text{XePd}_2\text{F}_{10}$ is shown in Fig. III-3. Its diamagnetism indicates a Xe(II):Pd(IV) complex.

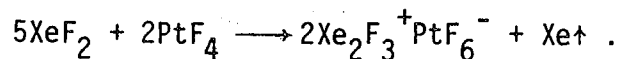
(d) Pyrolysis of $\text{XeF}_2 \cdot \text{PdF}_4$ with Formation of XeF_4 and Pd_2F_6

Thermal decomposition of $\text{XeF}_2 \cdot \text{PdF}_4$ at 280°C under vacuum produced pure XeF_4 and the mixed valent compound, $\text{Pd}^{\text{II}}\text{Pd}^{\text{IV}}\text{F}_6$. XeF_4 was characterized according to its X-ray powder photograph and Raman

spectrum. (See Fig. III-3.)

C. Results and Discussion

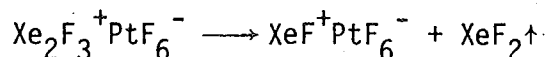
To favor the formation of XeF₂-rich complexes, and to encourage the development of crystalline material, PtF₄ was treated with a large excess of liquid XeF₂. It was quickly discovered that these mixtures generated xenon as the XeF₂ oxidized the Pt(IV) in an unanticipated reaction:



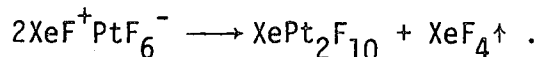
Removal of the excess XeF₂ provided the Pt(V) salt, Xe₂F₃⁺PtF₆⁻, which has previously been made² by mixing XeF₂ and PtF₅, in a 2:1 molar ratio, in BrF₅ solution:



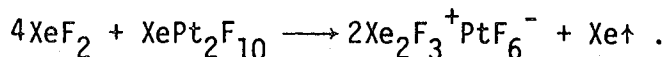
Our present findings establish that this salt loses XeF₂ under vacuum at ~ 70°C:



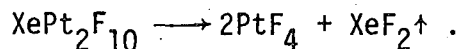
The compound XeF⁺PtF₆⁻, formed in this process, had also been prepared from XeF₂ and PtF₅ in BrF₅ solution and was well characterized structurally.² Pyrolysis of the compound at 160°C in a vacuum yielded XeF₄ and XePt₂F₁₀:



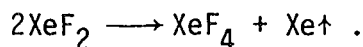
The XePt₂F₁₀ proved to be identical with the material of the same composition obtained by Bartlett and Jha.¹ Treatment of the XePt₂F₁₀ with excess liquid XeF₂ at 140-150°C again brought about oxidation of the Pt(IV) to Pt(V):



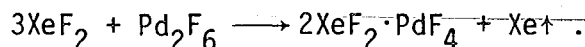
The pyrolysis of $\text{XePt}_2\text{F}_{10}$, under vacuum at 430°C , yielded no XeF_4 , but XeF_2 was evolved:



The combination of the oxidation of Pt(IV) to Pt(V), by the XeF_2 , with the Xe(II) oxidation to Xe(IV) by the Pt(V), has the net effect, as Fig. III-4 summarizes, of providing for the conversion of the two moles of XeF_2 to one of XeF_4 and one of Xe:

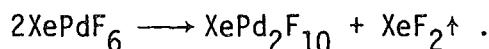


The interaction of liquid XeF_2 at $140\text{--}150^\circ\text{C}$ with PdF_4 yielded a diamagnetic yellow material. Changes in slope in a weight loss versus time curve indicated that 4:1, 3:1, 2:1 and 1:1 $\text{XeF}_2\text{:PdF}_4$ complexes probably occur; however, all but the 1:1 complex lose XeF_2 at or below 20°C . Our experience with the $\text{XeF}_2\text{/PtF}_4$ system suggested that liquid XeF_2 might prove capable of oxidizing the mixed valence palladium fluoride Pd_2F_6 and this proved to be so:

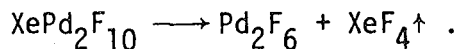


(This is convenient since Pd_2F_6 is much easier to prepare⁴ than PdF_4 .)

The 1:1 complex, XePdF_6 , loses XeF_2 in a vacuum at $140\text{--}150^\circ\text{C}$:



The solid residue, $\text{XePd}_2\text{F}_{10}$, proved to be a close structural relative of $\text{XePt}_2\text{F}_{10}$ (see below), but its pyrolysis proceeded quite differently. Like $\text{XePt}_2\text{F}_{10}$, $\text{XePd}_2\text{F}_{10}$ is rather stable thermally, but pyrolysis of $\text{XePd}_2\text{F}_{10}$ in a vacuum, at 280°C , yields XeF_4 :



The net effect of summing these reactions is again to provide for

the conversion of XeF_2 into XeF_4 and Xe, as Fig. III-5 illustrates.

The differences in the conditions which bring about the oxidation of Pt(IV) to Pt(V) by XeF_2 and those which bring about the reduction of Pt(V) to Pt(IV) by XeF_2 , are small. It is evident that if there is any thermodynamic obstacle to disproportionation it is not large. Although there are significant differences among the various values quoted⁵ for the enthalpies of formation of XeF_2 and XeF_4 , a set of calorimetric data, from one laboratory,⁶ indicates that the standard enthalpy change $\Delta H^\circ(2\text{XeF}_2(\text{g}) \longrightarrow \text{Xe}(\text{g}) + \text{XeF}_4(\text{g}))$ is $1.9 \text{ kcal mole}^{-1}$. The corresponding standard entropy change⁵ is $-9 \text{ cal deg.}^{-1} \text{ mole}^{-1}$. Thus the gaseous difluoride molecule is stable (although not greatly so) toward disproportionation and the more so the higher the temperature. Because the heats of sublimation⁷ of $\text{XeF}_2(\text{c})$ and $\text{XeF}_4(\text{c})$ are respectively 13.5 and 14.8 kcal mole⁻¹, $\Delta H^\circ(2\text{XeF}_2(\text{c}) \longrightarrow \text{Xe}(\text{g}) + \text{XeF}_4(\text{c})) = +13.5 \text{ kcal mole}^{-1}$. This is much less favorable for disproportionation than the gaseous-molecule case, although the corresponding standard entropy change⁵ is $+16.7 \text{ cal. del.}^{-1} \text{ mole}^{-1}$. It is probable that condensed-phase disproportionation of XeF_2 would be aided by the formation of the $\text{XeF}_2 \cdot \text{XeF}_4$ adduct,⁸ since the enthalpy of formation of this must be exothermic. Therefore, the value of $\Delta H^\circ(3\text{XeF}_2(\text{c}) \longrightarrow \text{Xe}(\text{g}) + \text{XeF}_2 \cdot \text{XeF}_4(\text{c}))$ is probably less endothermic than $13.5 \text{ kcal mole}^{-1}$ and could conceivably be exothermic. However, $\text{XeF}_2 \cdot \text{XeF}_4$ plays no part in the cycles presented here. Evidently the small amount of work necessary to drive the conversion of XeF_2 to XeF_4 is accumulated in the cycles.

The initial product in the PtF_4 oxidation by liquid XeF_2 is the salt $\text{Xe}_2\text{F}_3^+ \text{PtF}_6^-$. Here XeF_2 serves both as a fluoride ion donor² and

as an oxidizer. The anion in this salt does not interact strongly with the planar symmetrical V-shaped $(F-Xe \cdots F \cdots Xe-F)^+$ ion. When XeF_2 is removed from the $Xe_2F_3^+$ salt (and appreciable work is presumably done in this process), the anion is then subjected to the highly polarizing XeF^+ ion. The crystal structure of $XeF^+RuF_6^-$, which is a close relative of $XeF^+PtF_6^-$ (see X-ray data, Table III-5), indicates⁹ the anion-distorting nature of this cation-anion interaction. The Raman spectra in Fig. III-2 also give evidence of this change. It will be noted that the ν_3 -related mode, which is formally forbidden in the octahedral case, is not seen in $Xe_2F_3^+PtF_6^-$ but appears strongly in $XeF^+PtF_6^-$. Also, ν_5 in $XeF^+PtF_6^-$ is a doublet whereas in $Xe_2F_3^+PtF_6^-$ it is a singlet. There are also appreciable changes in the anion-stretching frequencies from one salt to the other. In $Xe_2F_3^+$, each Xe atom has two F atom neighbors coordinated approximately linearly to it and the electron-attracting capability, which such a Xe atom has, is much less than in the XeF^+ case. Indeed, the consequence of the interaction of XeF^+ , with one of the F-ligands of the anion, is to denude that ligand, and the anion as a whole, of some electron density. The Pt(V) in $XeF^+PtF_6^-$, because of its greater electronegativity is, potentially at least, a better oxidizer than the Pt(V) in $Xe_2F_3^+PtF_6^-$.

As in the platinum case, the fluoride ion donor capability of XeF_2 , coupled with its oxidizing capability, are responsible for the oxidation of Pd_2F_6 . The product in liquid XeF_2 is probably the salt $(Xe_2F_3^+)_2PdF_6^{2-}$. The yellow color is characteristic of PdF_6^{2-} salts and the XeF_6 analogue, $4XeF_6 \cdot PdF_4$ is known¹⁰ to be the salt $(Xe_2F_{11}^+)_2PdF_6^{2-}$. The electronegativity and oxidizing power of Pd(IV) in PdF_6^{2-} must be lower than in any

other Pd(IV) fluorospecies.

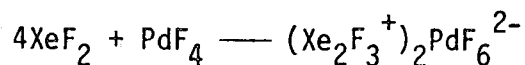
In the absence of reliable structural data for $\text{XeF}_2 \cdot \text{PdF}_4$, educated guesses are made as to its structure. In all XeF_2 complexes with fluoride ion acceptors, where the XeF_2 is not in molar excess, the combined X-ray crystallographic^{9,11} and vibrational spectroscopic evidence^{2,12} show the xenon-containing species to be XeF^+ . It is therefore expected that $\text{XeF}_2 \cdot \text{PdF}_4$ is an XeF^+ salt. A monomeric anion PdF_5^- is, however, not anticipated. In PdF_2 ,¹³ Pd_2F_6 ^{4,14} and PdF_4 ,⁴ the palladium atom is always octahedrally coordinated by F-ligands. In PdF_2 and Pd_2F_6 , the ligands are all equivalent but in PdF_4 , two adjacent F-ligands in the octahedron are uniquely associated with the central Pd-atom, whereas the other four ligands are each shared between two Pd atoms. This F-bridging in PdF_4 generates a three-dimensional lattice and a similar structure is adopted by RhF_4 , IrF_4 and PtF_4 .⁴ Although there is as yet no known pentafluoride of palladium, the pentafluorides of Rh, Ir, and Pt are all known and have the same structure. A precise version of this has been described¹⁵ for rhodium pentafluoride. The molecular unit shown in Fig. III-6 is a fluorine-bridged cyclic tetramer in which each Rh atom is octahedrally coordinated in F atoms. The anticipated PdF_5^- entity in $\text{XeF}_2 \cdot \text{PdF}_4$ may be similar. It is anticipated that the XeF^+ cation, as in the $\text{XeF}^+\text{MF}_6^-$ salts, will interact strongly with that anion.

The close structural relationship of $\text{XePd}_2\text{F}_{10}$ to $\text{XePt}_2\text{F}_{10}$ is supported by the X-ray powder data given in Table III-4. One can be confident that essentially the same heavy atom dispositions occur in both compounds. The Raman spectra, furthermore, which are shown in

Fig. III-3, give evidence of an XeF^+ species. That species is characterized² in the $\text{XeF}^+\text{MF}_6^-$ and $\text{XeF}^+\text{M}_2\text{F}_{11}^-$ salts by a band, or pair of bands, in the region $621\text{-}598\text{ cm}^{-1}$. The occurrence of a band at $\sim 610\text{ cm}^{-1}$ in each of the $\text{XeM}_2\text{F}_{10}$ spectra suggests that XeF^+ is a common component. See also Table III-4. There is little likelihood, however, of the anion being M_2F_9^- since again octahedral coordination of M is anticipated and a face-sharing of two octahedra has never been confirmed for any polyfluorometal species. The μ fluoro-bridged noble metal pentafluoride and tetrafluoride structures^{15,4} suggest that such an anion would involve each metal atom in μ -fluorobridging to three other metal atoms. This can give rise to an infinite polymer, but a discrete species could also occur, the simplest of which we would expect to be $\text{M}_8\text{F}_{36}^{4-}$. Such a species can be represented in terms of a distorted cube having M atoms at the corners, 12 bridging F-ligands in the edges (M-F-M angles $\neq 180^\circ$) and three unique F atoms per M atom completing the octahedral coordination of each M atom. Such a species can be formed by combining two superimposed $\text{RhF}_5)_4$ type units (see Fig. III-6). Whatever the structure of the anion, it appears, from the similarity of the Raman spectra of $\text{XeF}_6 \cdot 2\text{PdF}_4$ and $\text{XePd}_2\text{F}_{10}$ ($\text{XeF}_2 \cdot 2\text{PdF}_4$) (the data for which are in Table III-6) that the same form occurs in both compounds.

Since the breakup of the $\text{XePd}_2\text{F}_{10}$ lattice in vacuo at 280°C yields XeF_4 , it is evident that sufficient activation energy is available for the redox process at that temperature. In the interaction of liquid XeF_2 with PdF_4 at 140°C , the thermal energy may fall short of that necessary to activate the redox process, but it is more likely that the redox course is not followed simply because the XeF_2 , acting as a

fluorobase, quickly stabilizes the Pd(IV) as the PdF_6^{2-} ion:

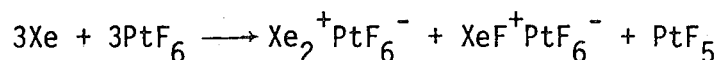


The decomposition of $\text{XePt}_2\text{F}_{10}$ takes a different course to that of $\text{XePd}_2\text{F}_{10}$ because Pt(IV) is much less oxidizing than Pd(IV) in an equivalent situation. This in itself is simply a consequence of the tighter binding of the valence electrons of Pd compared with Pt.

These studies have provided new and unexpected insights into a long-standing problem. The question concerning the constitution of XePtF_6 remains, however. The subtle interrelationships of the platinum and xenon oxidation states which this work has revealed allows for both Xe(I)Pt(V)F_6 and Xe(II)Pt(IV)F_6 formulations. Fortunately, the method described under Experimental provides material with a composition close to the 1:1 stoichiometry, XePtF_6 . The infrared spectrum of this material shown in Fig. III-1 indicates Pt(V) and is similar to the infrared spectrum of $\text{O}_2^+\text{PtF}_6^-$.¹⁶ Coincidentally, both XePtF_6 and XePdF_6 ($\text{XeF}_2 \cdot \text{PdF}_4$) are amorphous to X-rays (whereas $\text{XeF}^+\text{PtF}_6^-$ always reveals its presence by its characteristic X-ray pattern whenever the stoichiometry of the $\text{Xe} + \text{PtF}_6$ reaction product significantly exceeds 1:1). This gives rise to a suspicion that the poor crystal-developing character of both XePtF_6 and XePdF_6 could signify a structural relationship. However, magnetic measurements for approximately 1:1, XePtF_6 , suggest that this material may be ferrimagnetic whereas XePdF_6 is diamagnetic. Moreover, the close similarity of the infrared spectra of XePtF_6 and $\text{O}_2^+\text{PtF}_6^-$ is persuasive of the former like the latter being a PtF_6^- salt.

The xenon analysis of several samples of the Xe/PtF_6 reaction products indicate the difficulty of obtaining a 1:1 molar ratio of Xe to

PtF₆. All of the samples analyzed in this work, with the exception of the final one, show the % xenon less than required for Xe:PtF₆. Bartlett and Jha¹ also reported a ratio in which the Xe was in excess of PtF₆ in one of their tensimetric experiments. This high xenon content could indicate the presence of the dioxenon cation. This ion,¹⁸ recently characterized by oxidation of xenon with dioxygenyl salts, has a reported stretching frequency of 123 cm⁻¹. Lee and his coworkers¹⁷ have shown by direct photoionization studies that the Xe₂⁺ ion has a dissociation energy of approximately 23 kcal/mole. It should be appreciated, however, that this ion could be formed and still maintain the 1:1 stoichiometry as the following reaction indicates:



The complexity of the infrared spectrum shown in Fig. III-1 could be compatible with such a mixture of products. It is clear that further investigations are necessary.

TABLE III-1

Experimental data for the XeF ₂ /Platinum fluoride and XeF ₂ /palladium fluoride systems		
Reactants	Conditions	Products and Characterization
Mix: PtF ₄ 0.4253 g 1.57 mmole XeF ₂ 1.8138 g 10.71 mmole	140-150° for ~ 48 hr, then evacuated at -80° excess XeF ₂ removed <u>in vacuo</u> at ~ 20°	volatile: Xe (no IR, condensible -196°) 0.0995 g 0.76 mmole yellow solid (p): Xe ₂ F ₃ PtF ₆ (X-R1, R1) 0.938 g 1.49 mmole
Xe ₂ F ₃ PtF ₆ 0.8893 g 1.41 mmole	~ 70° in vacuo for 17 hrs	orange-yellow solid (p): XeFPtF ₆ (X-R2, R2) 0.6422 1.40 mmole
XeFPtF ₆ 0.3711 g 0.81 mmole	~ 140° <u>in vacuo</u> for several hours	volatile: XeF ₂ (IR1) caught in -196° trap red-brown solid (d): XePt ₂ F ₁₀ (X-R3, R3) 0.2947 g 0.41 mmole
XePt ₂ F ₁₀ 0.1142 g 0.16 mmole	~ 430° <u>in vacuo</u> for several hours	volatile: XeF ₄ (IR2) caught in -196° trap light brown solid (d): PtF ₄ (X-R4, R4) 0.0771 g 0.28 mmole
Mix: Pd ₂ F ₆ (1) 0.50 1.53 XeF ₂ 2.96 17.48	142° for 11 hr, then evacuated at - 80° excess XeF ₂ removed <u>in vacuo</u> * at ~ 20° to constant weight	volatile: Xe (no IR, condensible -196°) (1) 0.19 g (2) 0.192 g 1.45 mmole 1.46 mmole yellow solid (d): XePdF ₆ (R5, IR3) (amorphous to X-R) 1.0228 g 2.91 mmole

TABLE III-1 (continued)

Reactants	Conditions	Products and Characterization
Mix: PdF ₄ 0.271 g 1.49 mmole XeF ₂ 1.480 g 8.74 mmole	150° for 48 hr, excess XeF ₂ removed at ~ 20° to constant weight*	yellow solid as above: XePdF ₆ (R5, IR3) 0.54 g 1.54 mmole
XePdF ₆ 1.0228 g 2.91 mmole	140-150 <u>in vacuo</u> for several hours	light brown to pink solid (d): XePd ₂ F ₁₀ (X-R5, R6) 0.7513 g 1.41 mmole volatile: XeF ₂ (IR1) caught in -196° trap
XePd ₂ F ₁₀ 0.3489 g 0.65 mmole	280° <u>in vacuo</u> for 2 hr	black solid (p): Pd ₂ F ₆ (X-R6) 0.2234 g 0.68 mmole volatile: XeF ₄ (IR2) caught in -196° trap

p-paramagnetic; d-diamagnetic

X-ray powder data: X-R1 in Table III-2; X-R2 in Table III-5; X-R3 and 5 in Table III-4 and X-R4 in ref. [4]; X-R6 in ref. [14], where Pd₂F₆ is described as PdF₃.

Raman data: R1 and R2 in Fig. III-2, R3, 4, and 6 in Fig. III-3, R5-see Table III-3.

Infrared data: for IR1 and 2 see book cited in ref. [1]. For IR3 see Table III-3.

*Weight-loss time curves for the x XeF₂·PdF₄ material indicated the phases 4XeF₂·PdF₄; 3XeF₂·PdF₄; 2XeF₂·PdF₄ and the 1:1 compound.

TABLE III-2. X-ray powder data for $\text{Xe}_2\text{F}_3^+\text{PtF}_6^-$ and related salts

$\text{Xe}_2\text{F}_3^+\text{IrF}_6^-$		$\text{Xe}_2\text{F}_3^+\text{PtF}_6^-$		$\text{Xe}_2\text{F}_3^+\text{RuF}_6^-$	
$10^4 \frac{1}{d^2}$	I/I ₀	$10^4 \frac{1}{d^2}$	I/I ₀	$10^4 \frac{1}{d^2}$	I/I ₀
596	vs	582	vs	596	s
647	vs	642	vs	654	s
693	s	690	s	695	s
726	mw				
811	vs	806	vs	811	s
878	vs	875	vs	883	s
1052	ms	1054	mw	1057	vW
1437	mw				
1513	mw	1507	w		
1715	s	1714	s		
				1744	ms
1814	mw	1789	VVW		
1865	s	1851	ms		
1969	ms	1933	mw	1956	vW
2200	ms	2175	mw	2222	vW
2308	s	2290	s	2330	ms
		2499	w	2515	VVW
2765	s	2754	mw	2911	mw
3221	s	3197	s	3246	mw
		3709	VVW		
3860	w	3846	vW		
				3906	VVW
4019	w				
4049	w	4030	w	4060	VVW
4185	w				
5295	s			5344	mw
5415	w				
5586	w				
5857	vW				
6690	w				
7230	w				

vs > s > ms > m > mw > w > vW > VVW

TABLE III-3. Raman and infrared bands for $\text{XeF}_2 \cdot \text{PdF}_4$

R(cm^{-1})*		649(9)	585(2)	505(1)	385(1)	230(1)
IR(cm^{-1})	655(sh)	635(vs)	580(s)		470(s)	

*All Raman bands were very broad; relative intensities are given in parentheses.

TABLE III-4. X-ray powder data for $\text{XeF}_2 \cdot 2\text{PdF}_4$ and $\text{XeF}_2 \cdot 2\text{PtF}_4$

$\text{XeF}_2 \cdot 2\text{PdF}_4$		$\text{XeF}_2 \cdot 2\text{PtF}_4$	
$10^4 \frac{1}{d^2}$	I/I ₀	$10^4 \frac{1}{d^2}$	I/I ₀
140	m	153	w
-	-	185	w
-	-	417	vW
-	-	458	vW
515	vW	529	vW
580	vS	588	s
670	s	672	vS
-	-	691	vW
-	-	777	m
837	vS	847	vS
953	vS	958	vS
1081	vW	1075	w
-	-	1116	vW
1244	w	1235	w
-	-	1328	vW
1355	m	1386	m
1415	w	1451	vW
-	-	1504	vW
-	-	1599	vW
-	-	1626	vW
1728	w	1732	m
1869	m	1869	s
2046	w	2042	m
2096	vW	2103	m
2202	vW	2213	w

TABLE III-5. X-ray powder data for $\text{XeF}^+\text{PtF}_6^-$ and $\text{XeF}^+\text{RuF}_6^-$

XeFPtF_6			XeFRuF_6			hkl
I/I_0	$10^4 \frac{1}{d^2}_{\text{obs}}$	$10^4 \frac{1}{d^2}_{\text{calc}}$	I/I_0	$10^4 \frac{1}{d^2}_{\text{obs}}$	$\frac{1}{d^2}_{\text{calc}}$	
	-	437	m	429	{ 424 432	$\bar{1}11$ 111
m	489	487	ms	480	482	120
s	632	632	s	629	627	200
vs	687	684	vs	674	{ 667 675	$\bar{1}21$ 121
m	788	787	ms	762	761	002
mw	871	869	ms	839	842	012
	-	938	w	923	923	031
vw	1020	1027	w	999	{ 990 1007	$\bar{1}12$ 112
vw	1111	1096	w	1084	{ 1075 1083 1086	$\bar{1}31$ 131 022
		1116	w	1251	{ 1234 1250	$\bar{1}22$ 122
	-	1317	w	1304	1302	040
m	1394	1373	w	1364	1359	230
m	1479	1475	m	1452	1459	140

* $\frac{1}{d^2}$ calculated for XeFPtF_6 assuming $\beta = 90^\circ$. Found $a = 7.96$, $b = 11.02$, $c = 7.13$ Å.

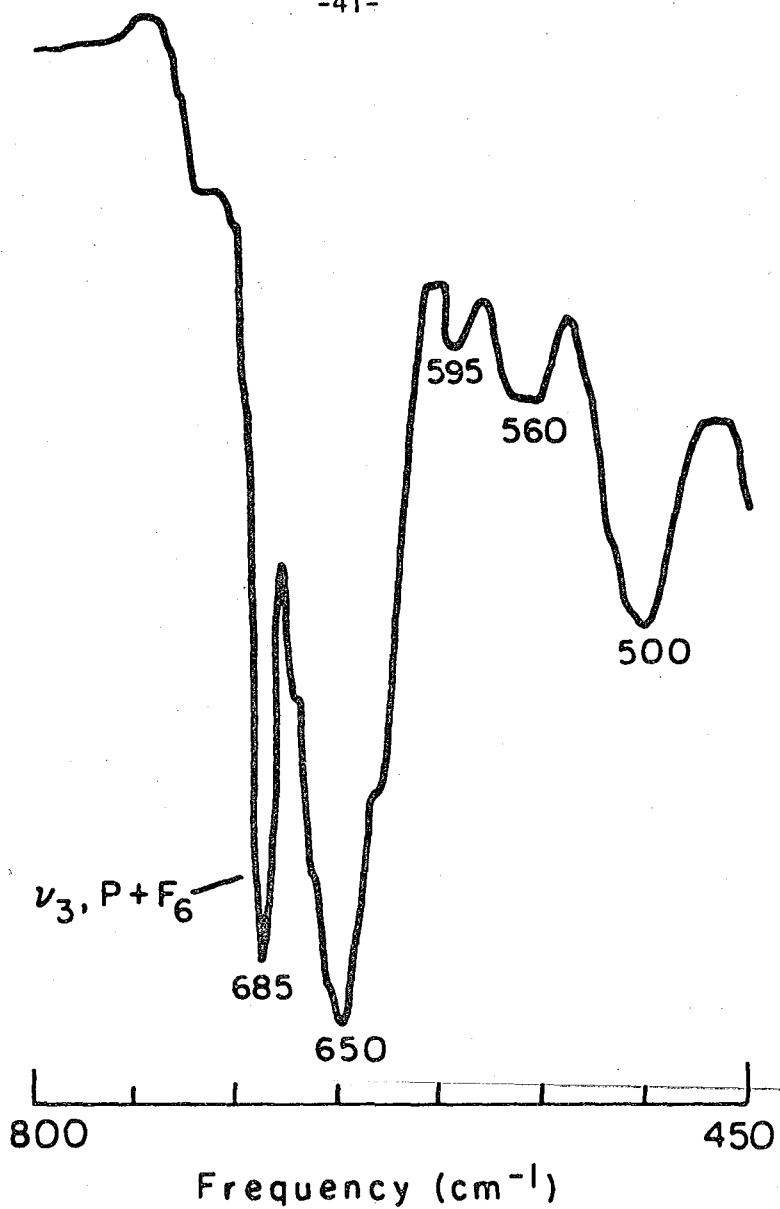
**The $\frac{1}{d^2}$ calc values for XeFRuF_6 are from the cell dimensions obtained in the single crystal study in ref. [9].

TABLE III-6. Raman shifts (cm^{-1}) for $\text{XeF}_2 \cdot 2\text{PdF}_4$ and $\text{XeF}_6 \cdot 2\text{PdF}_4$

XeF^{+*} in XeFPtF_6	$\text{XeF}_2 \cdot 2\text{PdF}_4$	$\text{XeF}_6 \cdot 2\text{PdF}_4$	XeF_5^{+**} in $(\text{XeF}_5)_2\text{PdF}_6$
		686(1) {676(3), 660(5)} ν_7
		679(1) 653(100) ν_1
	652(7) 659(7)	
	647(sh,2) 649(5)	
	636(sh,1) 639(sh,2)	
		625(2)	
		618(2) 606(2), ν_4
609, 602} 610(1)		
		608(3) 590(71), ν_2
	583(1)		
	562(<1)} 567(1)	
	553(1)		
		408(2) 425(3)
		404(sh,2) 396(sh)} ν_8
	392(1) 397(sh,1)	
	320(<1)		
		302(1) 309(10), ν_3
	283(<1) 296(1)	
	269(<1) 273(2)	
	259(<1) 258(1)	
	244(<1) 243(1)	
	238(1) 231(1)	
	197(<1) 215(<1)	
	185(<1) 185(1)	

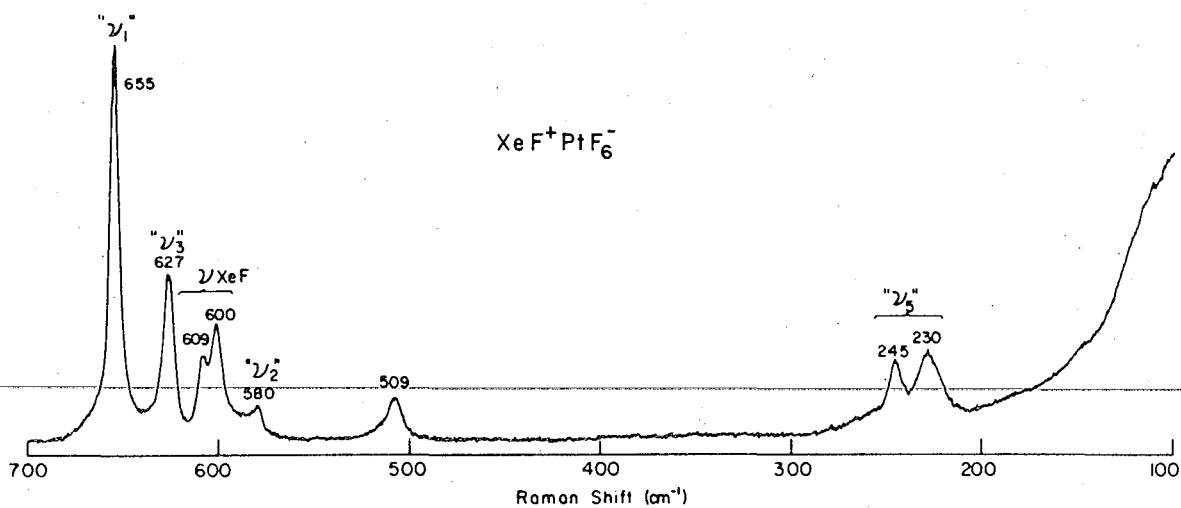
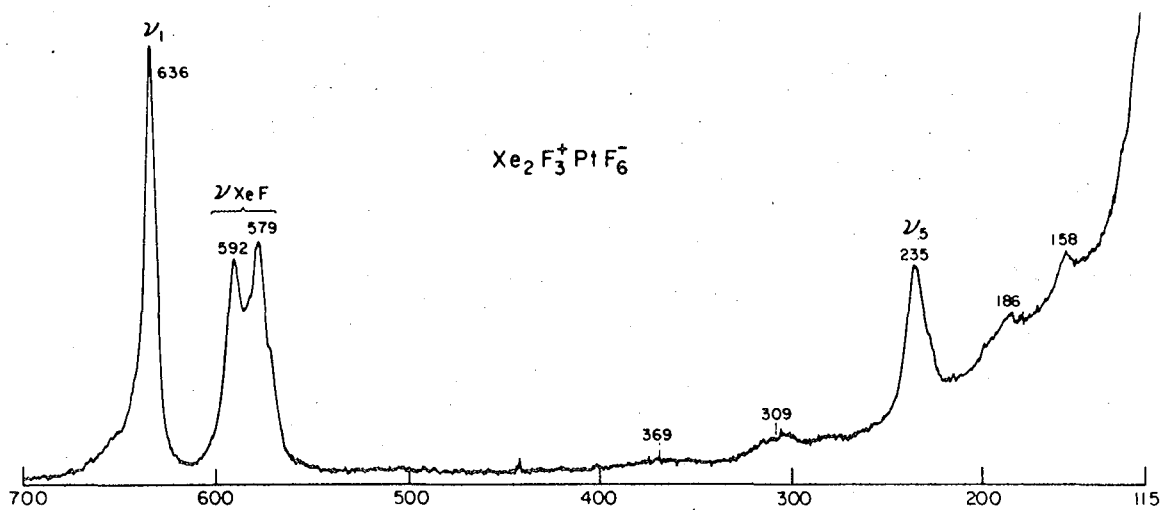
*Rev. [2].

**C.J. Adams and N. Bartlett, Israel J. Chem. 17, 114 (1978).



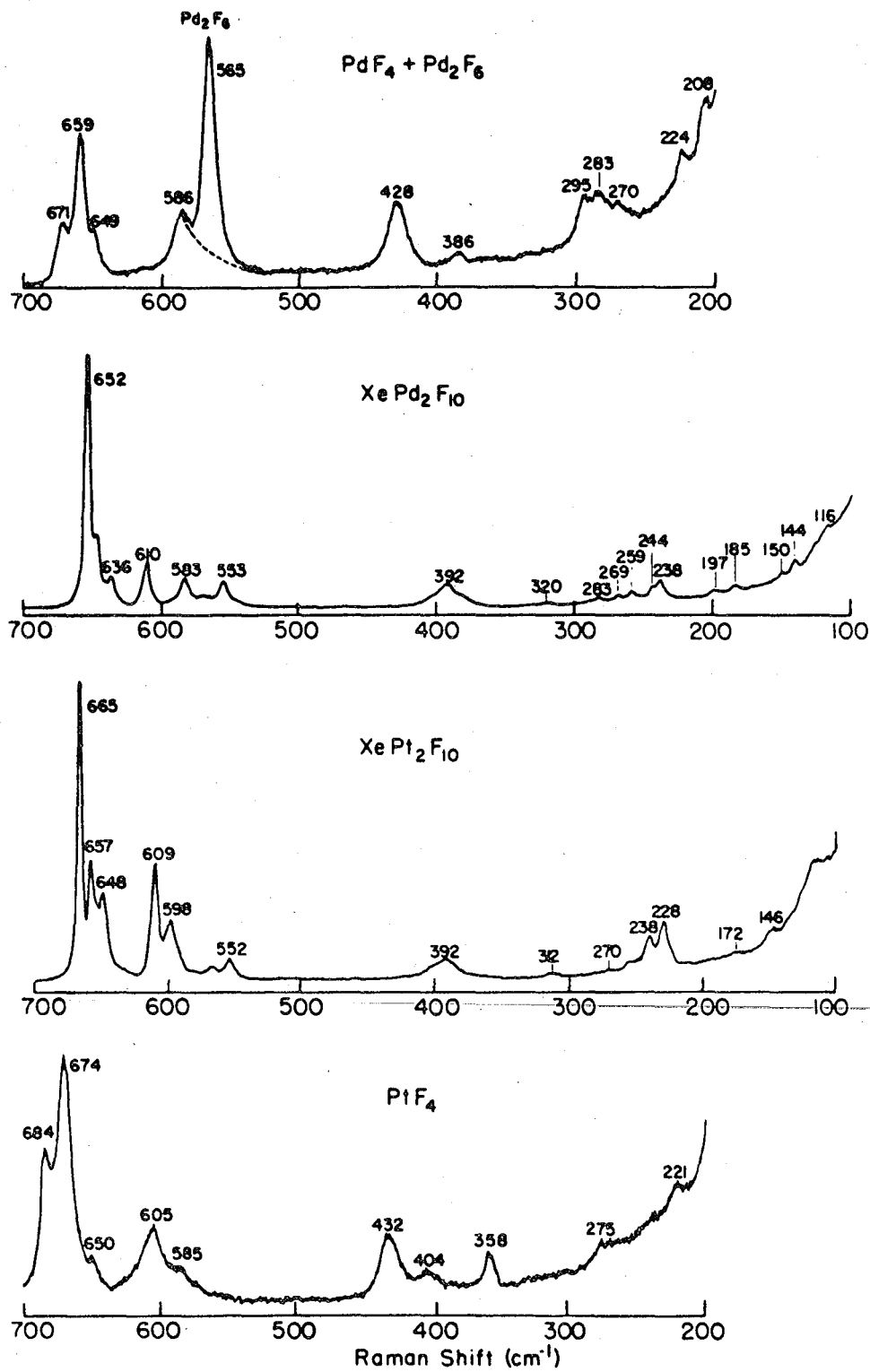
XBL 788-5679

Figure III-1. Infrared spectrum of the Xe + PtF₆ reaction product(s) at 10°K.



XBL 759-735I

Figure III-2. Raman spectra of $\text{Xe}_2\text{F}_3^+\text{PtF}_6^-$ and $\text{XeF}^+\text{PtF}_6^-$.



XBL 759-7352

Figure III-3. Raman spectra of PdF₄, Pd₂F₆, XeF₂·2PdF₄, XeF₂·2PtF₄ and PtF₄.

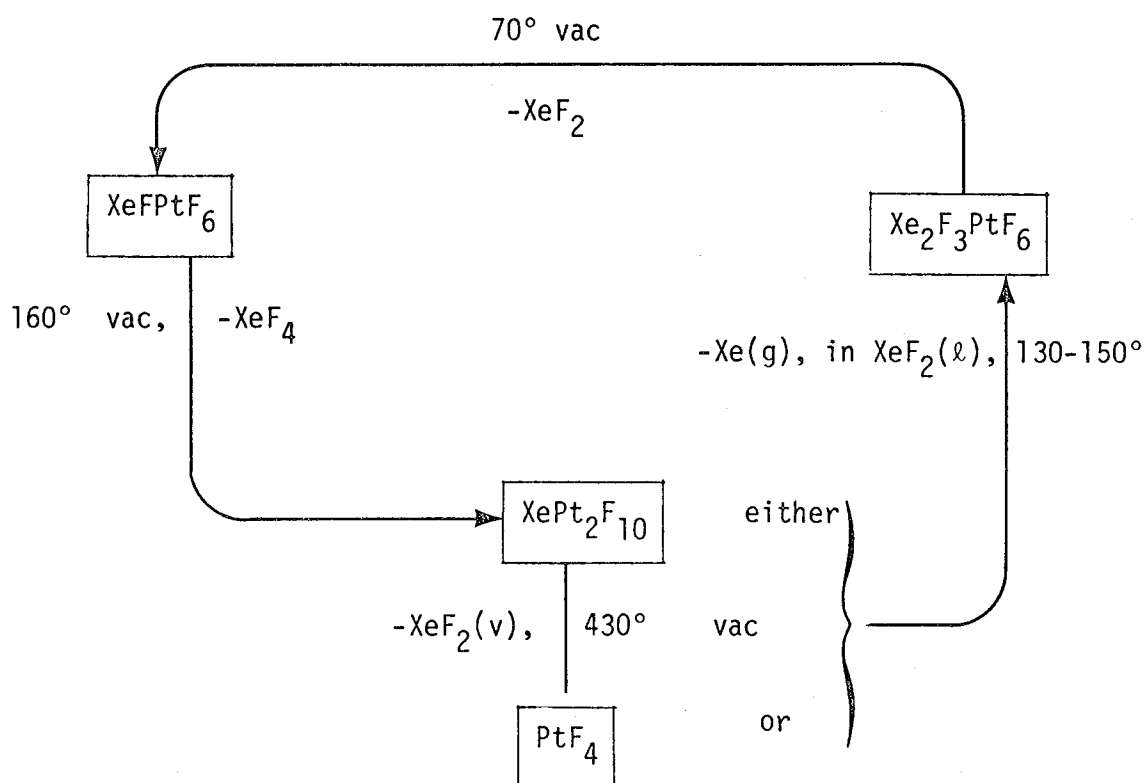


Figure III-4. Conversion of XeF₂ to XeF₄ + Xe using platinum fluorides.

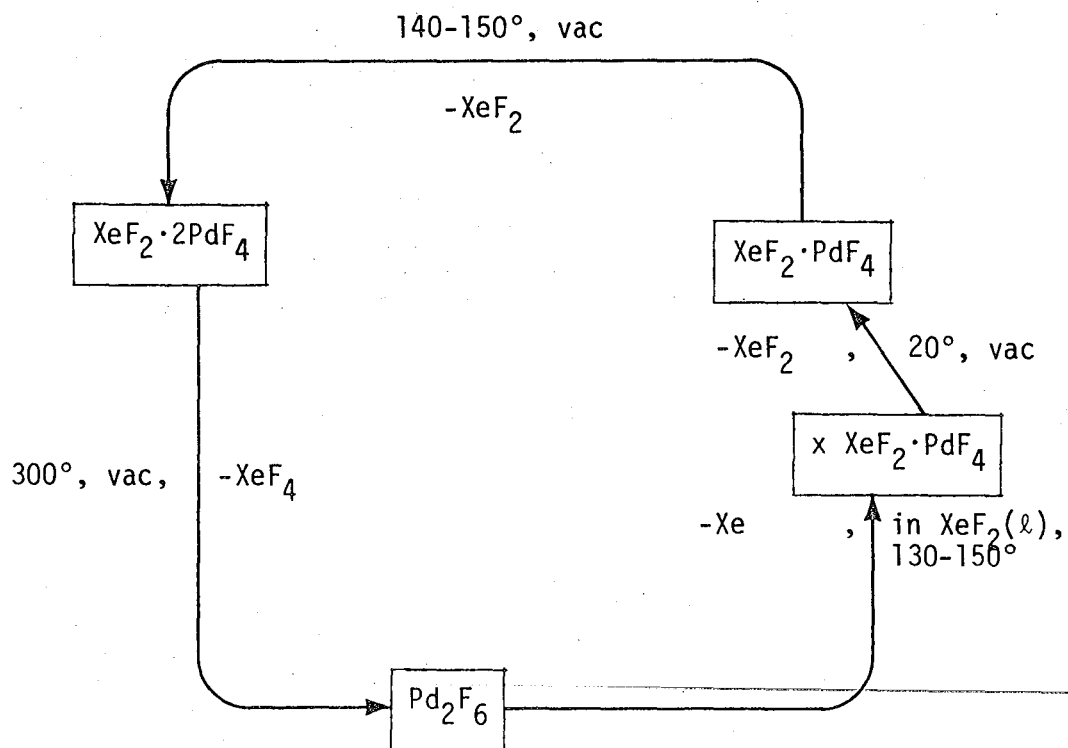


Figure III-5. Conversion of XeF₂ to XeF₄ + Xe using palladium fluorides.

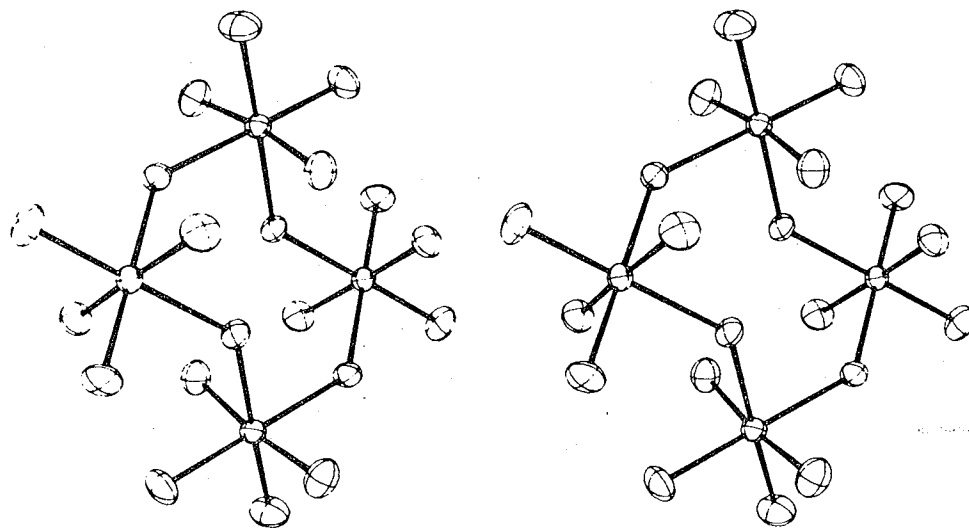
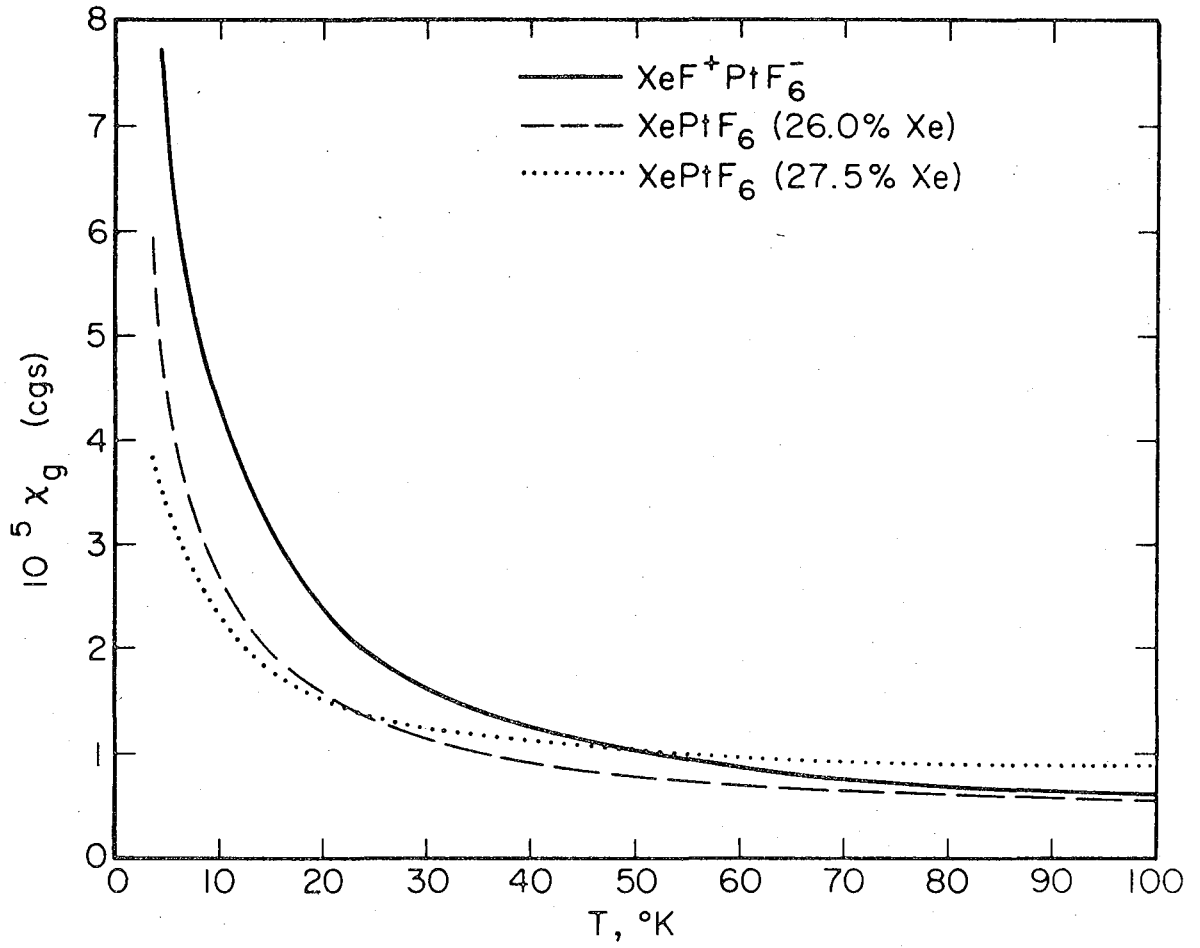


Figure III-6. The RhF₅ tetramer.....a possible model for (PdF₅⁻).



XBL-788-10628

Figure III-7. $10^5 X_g$ vs T plot for $XeF^+PtF_6^-$, $XePtF_6$ (26.0% Xe) and $XePtF_6$ (27.5% Xe).

REFERENCES

1. N. Bartlett and N.K. Jha, Noble Gas Compounds, H.H. Hyman, ed., p. 23 ff. (University of Chicago Press, Chicago and London, 1963).
2. F.O. Sladky, P.A. Bulliner and N. Bartlett, J. Chem. Soc. (A), 2179 (1969).
3. N. Bartlett and J.W. Quail, J. Chem. Soc., 3728 (1961).
4. N. Bartlett and P.R. Rao, Proc. Chem. Soc., 393 (1964) and P.R. Rao, A. Tressaud and N. Bartlett, J. Inorg. and Nucl. Chem., Supplement, 23 (1976).
5. N. Bartlett and F.O. Sladky, The Chemistry of Krypton, Radon and Xenon in Comprehensive Inorganic Chemistry, J.C. Bailor, Jr., et al, eds. (Pergamon Press, 1973), Vol. 1, p. 213 ff.
6. G.K. Johnson, J.G. Malm and W.W. Hubbard, J. Chem. Thermodynamics 4, 879 (1972).
7. F. Schreiner, G.N. McDonald and C.L. Chernik, J. Phys. Chem. 72, 1162 (1968).
8. J.H. Burns, R.D. Ellison and H.H. Levy, Acta Cryst. 18, 11 (1965).
9. N. Bartlett, M. Gernis, D.D. Gibler, B.K. Morrell and A. Zalkin, Inorg. Chem. 12, 1717 (1973).
10. K. Leary, A. Zalkin and N. Bartlett, Inorg. Chem. 13, 775 (1974).
11. V.M. McRae, R.D. Peacock and D.R. Russell, Chem. Comm., 1048 (1968).
12. R.J. Gillespie, A. Netzer and G.J. Schrobilgen, Inorg. Chem. 13, 1455 (1974).
13. N. Bartlett and R. Maitland, Acta Cryst. 11, 747 (1958).
14. M.A. Hepworth, K.H. Jack, R.D. Peacock and G.J. Westland, Acta Cryst. 10, 63 (1957).
15. B.K. Morrell, A. Zalkin, J. Tressaud and N. Bartlett, Inorg. Chem. 12, 2640 (1973).
16. N. Bartlett and D.H. Lohmann, J. Chem. Soc., 5253 (1962).
17. C.Y. Ng, D.J. Trevor, B.H. Mahan and Y.T. Lee, J. Chem. Phys. 65, 4327 (1976).

18. L. Stein, J.R. Norris, A.J. Downs and A.R. Minihan, Chem. Comm., 502 (1978).

IV. THE INTERACTION OF CHLORINE WITH THE THIRD-SERIES TRANSITION METAL HEXAFLUORIDES AND RELATED STUDIES

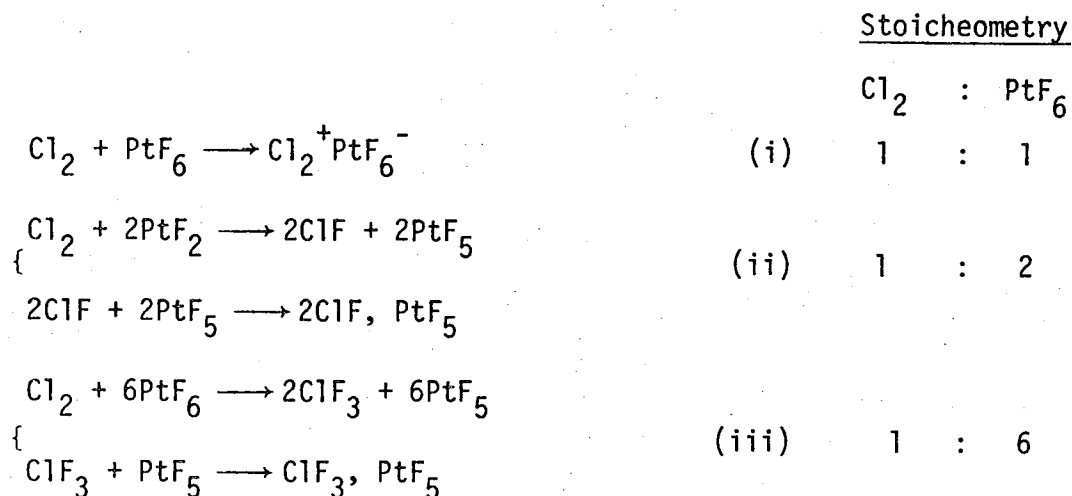
A. Introduction

The Cl_2^+ radical cation, with a stretching frequency of 645.3 cm^{-1} , has been identified only in the gas phase at low pressures.¹ Claims by Olah and Comisarow for the existence of Cl_2^+ and ClF^+ in solution^{2,3} on the basis of esr spectra observed for solutions of chlorine fluorides in SbF_5 , $\text{HSO}_3\text{F-SbF}_5$ or HF-SbF_5 have been criticized by several workers. Eachus, Sleight and Symons,⁴ argued that the esr spectrum attributed to ClF^+ could be ascribed to ClOF^+ since the esr parameters agreed well with those of isoelectronic and pseudo-isoelectronic radicals such as ClO_2 , FOO and NF_2 . By analogy they assigned the esr spectrum attributed to Cl_2^+ by Olah and Comisarow to the ClOCl^+ cation. Christie and Muirhead⁵ showed that neither ClF^+ nor Cl_2^+ radicals, as reported by Olah et al, were produced in the above solutions if care was taken in purification of the reactants. They concluded that the spectra observed by Olah were due to impurities. Further support for oxy-radicals was given by Gillespie and Morten.⁶ An increase in intensity was observed in the esr spectrum, which had been attributed to the ClF^+ ion, when a small amount of water was added to a sample of $\text{ClF}_2^+\text{SbF}_6^-$ in antimony pentafluoride.

The radical cations Br_2^+ and I_2^+ have, however, been prepared both in solid salts and in solution. The reaction of bromine, bromine pentafluoride and antimony pentafluoride was shown by Edwards, Jones and Sills⁷ to give the paramagnetic scarlet salt, $\text{Br}_2^+\text{Sb}_3\text{F}_{16}^-$. Moreover,

Gillespie and Morten,⁸ at the same time, reported the existence of the Br_2^+ cation in the fluorosulfuric acid solvent system. Gillespie and Milne showed⁹ that the oxidation of iodine using peroxydisulphuryl difluoride formed the blue iodine species I_2^+ and not I^+ as previously reported. Subsequently, Kemmitt et al¹⁰ reported the preparation of blue crystalline solids from iodine and antimony pentafluoride and tantalum pentafluoride. Blue solutions formed on addition of iodine to the Lewis acids SbF_5 , TaF_5 , NbF_5 , AsF_5 and PF_5 in iodine pentafluoride were also investigated by these authors. In all cases, their results were interpreted in terms of the I_2^+ radical cation. No satisfactory accounting for the oxidation of I_2 by these pentafluorides or indeed the similar oxidation of Br_2 by SbF_5 has been given; i.e., the reduction product was not identified in any of the cases.

Prior to the present studies, several workers had investigated mixtures of molecular chlorine and transition metal hexafluorides. Robinson and Westland confirmed earlier findings by Ruff and Fisher¹¹ that chlorine reacted with iridium hexafluoride at 55-60°C to yield an oil from which " IrF_4 " sublimed at 120-140°C. This material, thought to be IrF_4 by Robinson and Westland, was later identified by Bartlett and Rao as IrF_5 .¹² Subsequent, related studies by Jha,¹³ which were directed toward the preparation of Cl_2^+ salts, showed that chlorine reacted with platinum hexafluoride in the molar ratio of 1:2.5. The resultant solid was amorphous to X-rays, and the infrared spectrum of the volatiles showed no evidence for ClF , ClF_3 or ClF_5 . He proposed the following possible reactions:



with (i) and (ii) predominant.

Jha obtained an approximately 1:1 stoicheometry on reacting chlorine gas with iridium hexafluoride vapor at room temperature. Infrared spectroscopic evidence indicated that neither ClF nor ClF₃ gas was liberated in the reaction. He further observed that the pale yellow solid, formed initially, transformed into a deeper yellow liquid within a few minutes. This liquid transformed to a yellow solid in a few weeks and the latter was identified by X-ray photography as iridium pentafluoride. Since the final product was iridium pentafluoride and the reaction stoicheometry indicated an initial 1:1 Cl₂:IrF₆ compound, Jha assumed that the initial product was the quinquevalent iridium salt Cl₂⁺IrF₆⁻.

More recently Richardson¹⁴ reacted chlorine with dioxygenyl salts of arsenic and antimony in an attempt to use these materials as one electron oxidizers:

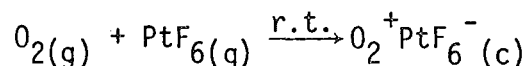


Thermally unstable, lavender-colored solids were formed with very little,

if any, oxygen evolution. The lavender solids remain to be characterized.

These earlier findings prompted us to investigate the $\text{Cl}_2:\text{MF}_6$ systems at even lower temperatures in an attempt to identify the Cl_2^+ radical cation in the crystalline state. The intermediate products resulting from the thermal decomposition of the initial $\text{Cl}_2:\text{IrF}_6$ interaction were also of interest.

The third-series transition metal hexafluorides are well known for their oxidizing ability. Bartlett had shown from comparative studies of these hexafluorides with nitric oxide, nitrosyl fluoride, xenon and oxygen that the electron affinity increased by approximately 1 eV with each unit change in Z as one proceeded from the left to the right of the periodic series.¹⁵ Platinum hexafluoride is the only known third transition series hexafluoride which can oxidize oxygen:^{16,17}



The first ionization potential of molecular oxygen is 281 kcal/mole (12.1 eV) compared to 265 kcal/mole (11.3 eV) for molecular chlorine.

Although the Cl_2^+ ion must be larger than O_2^+ and the lattice energy of a $\text{Cl}_2^+\text{MF}_6^-$ salt therefore appropriately lower than for the related O_2^+ salt, the more favorable ionization potential of Cl_2 compared with O_2 was anticipated to outweigh the lattice energy term. It appeared that platinum hexafluoride should be capable of oxidizing molecular chlorine. It even appeared to be possible that iridium hexafluoride could prove capable of oxidizing chlorine since the large MF_6^- ions have a leveling effect on the lattice energies with the result that the Cl_2^+ salt lattice energies are not more than 5 kcal mole⁻¹ less favorable than for the

O_2^+ salts.

A systematic study of molecular chlorine with the third-series transition metal hexafluorides was therefore undertaken.

B. Experimental

The chlorine plus transition metal hexafluoride reactions were studied using two quartz reactor types. The first, an elongated bulb, was made by joining an approximately 4 in. length of 3/8 in. diameter tubing to a second length (4 in.) of 1 in. diameter. This bulb was used when either measuring the stoichiometry of the initial chlorine-transition metal fluoride interaction or when monitoring the volatile thermal decomposition products. The second reactor was made by sealing a 3-4 in. length of 1/4 in. tubing to a 1 in. length of 1/4 x 3/8 in. rectangular cross-section tubing. This vessel served as a reactor and a good sample holder for Raman spectra. The open end of each reactor was joined to a brass IKS4 Whitey valve, via Swagelock compression fittings with teflon gaskets, a reducing union being also employed where appropriate.

1. The Cl_2/IrF_6 Studies

(a) The Stoichiometry of the $Cl_2:IrF_6$ Reaction

In a typical experiment, 250-600 mg. of iridium hexafluoride was combined with excess chlorine at $-196^\circ C$. Deep blue patches were observed along the wall of the quartz vessel. The mixture was then warmed toward room temperature ($\sim 25^\circ C$) with continuous agitation. When the pressure within the reactor reached approximately two atmospheres, it was cooled to $-80^\circ C$. At this point the blue coloration was observed

to be spread throughout the mixture. This warm/cool procedure (25° to -80°C) was repeated several times to ensure complete reaction of the metal hexafluoride. The blue coloration decreased in intensity following each warm/cool step. Excess chlorine was removed at -80°C to leave a pale yellow solid. The gravimetry and tensimetry measurements given in Table IV-1 indicated that the molar combining ratio of $\text{Cl}_2:\text{IrF}_6$ for this solid is approximately 1:1.

(b) Spectroscopic Studies of the Product of the Cl_2/IrF_6 Reaction

In the first vibrational spectroscopic studies, chlorine and iridium hexafluoride were deposited on to the cold silver block (ca. 10°K) and the AgCl window of the cryo-tip described under II-A. Typically a thin layer of chlorine was deposited on the cold-surface, followed by co-deposition from the two gases. A blue species was observed on the cold-surface a few minutes after the start of the co-deposition. The flow rate of the hexafluoride, which was usually less than that of the chlorine, was monitored using infrared spectroscopy in an attempt to deposit as little unreacted iridium hexafluoride as possible. The Raman and infrared spectra, shown in Figs. IV-1(a) and IV-2, respectively, were obtained after 4-5 hours deposition time. The sample was warmed approximately 15°, re-cooled and the spectrum monitored again. Warming above 190°K caused the blue species to disappear and the sample to fall from the cold-surface.

The Raman spectrum of the pale yellow solid prepared in the quartz reactor is also shown in Figure IV-1(b), since the two spectra have much in common. Both, however, contradict the measured stoichiometry. A

possible explanation for the observed spectra follows under Results and Discussion. Warmup of the pale yellow solid, prepared in the quartz bulb, to room temperature produced a gradual increase in its color intensity. The solid phase persisted for approximately one week at room temperature, after which it slowly decomposed to a dark yellow liquid. After a few weeks at room temperature, the liquid transformed to a crystalline yellow solid which proved to be iridium pentafluoride. This thermal decomposition of the initial product was monitored with infrared (see Figure IV-3) and Raman spectroscopy and is described under Results and Discussion.

(c) Reactions of the Cl_2/IrF_6 Products

The reaction chemistry of the Cl_2/IrF_6 products were monitored at three separate times: (1) immediately following the preparation of the $\text{Cl}_2:\text{IrF}_6$ initial product (sample kept at -80°C , pale yellow solid); (2) after 2-3 days at 23°C (bright yellow solid); (3) after approximately one week at 23°C (solid/liquid phase). The products of the $\text{Cl}_2:\text{IrF}_6$ reaction at these three times will be referred to later as initial, intermediate and solid/liquid phase products, respectively.

(i) Reaction with NO

An excess of NO was condensed onto the initial pale yellow Cl_2/IrF_6 reaction product at -196°C . The mixture was allowed to warm to room temperature, recooled, and warmed again. An infrared spectrum of the volatiles showed NO and NOCl. An X-ray powder photograph of the pale yellow residue showed predominantly $\text{NO}^+\text{IrF}_6^-$ with very weak lines due to the 2:1 salt, $(\text{NO}^+)_2\text{IrF}_6^{2-}$.^{13,18}

(ii) Reaction with C_6F_6 in WF_6

WF_6 , followed by C_6F_6 , was distilled onto the initial Cl_2/IrF_6 reaction product. The mixture was warmed slowly until melting and reaction occurred. Judicious cooling was necessary to moderate the very exothermic reaction. A pressure increase, presumably chlorine, in excess of one atmosphere was observed. Excess C_6F_6 and other volatiles were removed under vacuum at $0^\circ C$ leaving behind a yellow, free-flowing solid. Within the 15 to 20 minutes required to transfer the reactor into the Dri-lab, the solid had transformed into a reddish opalescent liquid. The Raman spectrum of this indicated the presence of poorly crystalline iridium pentafluoride. The infrared spectrum of the volatiles above the liquid showed CF_4 , C_2F_6 and other carbon fluorides. The liquid, upon standing several weeks at room temperature, changed to a bright yellow solid which proved to be crystalline iridium pentafluoride.

WF_6 and C_6F_6 were sequentially distilled into a sample of the solid/liquid phase product. No immediate pressure increase was observed at $23^\circ C$. Presumably the C_6F_6/WF_6 mixture served as a solvent for the solid-liquid interaction. C_6F_6 and WF_6 were removed at $0^\circ C$ leaving behind a crystalline yellow-orange solid. Its Raman spectrum is shown in Figure IV-4 and is discussed under Results and Discussion.

(iii) Reaction with BrF_3

BrF_3 was condensed into the quartz vessel containing the initial pale yellow solid at $-196^\circ C$. The temperature was increased slowly until melting of the bromine trifluoride occurred. The pressure increased very rapidly to 1300 torr. An infrared spectrum of the volatiles above the solid, now an even paler yellow, showed the

presence of chlorine monofluoride and some carbon tetrafluoride. The Raman spectrum of the volatiles, liquefied by cooling to -90°C , showed only chlorine and chlorine monofluoride. The yellow crystalline solid residue was examined by Raman spectroscopy at -80°C which indicated a $\text{BrF}_3 \cdot \text{IrF}_5$ complex which is assumed to be the 1:1 compound reported by Robinson and coworkers.¹⁹

An excess of BrF_3 was distilled onto a sample of the intermediate $\text{Cl}_2:\text{IrF}_6$ product at -196°C . The contents of the vessel were then allowed to warm slowly to 23°C . Again a significant increase in pressure was observed. Infrared monitoring of the volatiles showed only chlorine monofluoride. The yellow solid left in the reactor, on removal of volatiles at 23°C , proved to be identical to the product formed when BrF_3 was added to the initial $\text{Cl}_2:\text{IrF}_6$ reaction product.

(iv) Reaction with ClO_2F

An excess of chloryl fluoride, ClO_2F , was distilled onto a sample of the intermediate product contained in a quartz reactor at -196°C . A vigorous reaction ensued upon warming and agitating the mixture. Gas evolution was evident in the liquid ClO_2F at -80°C . An infrared spectrum of the volatiles, above a yellow solid, showed ClF and ClO_2F . The solid transformed, within one hour at 23°C , to a dark yellow liquid. Pumping off the liquid at 23°C resulted in the formation of an even deeper yellow solid. The Raman spectrum of this solid proved it to be iridium pentafluoride.

(v) Reaction with IF_5

Excess iodine pentafluoride, IF_5 , was condensed into a vessel containing the intermediate $\text{Cl}_2:\text{IrF}_6$ product at liquid N_2

temperature. An intense green color was observed on warming the mixture to 23°C. An infrared spectrum of the volatiles, however, showed only IF_5 . The green color became less intense upon pumping until it finally disappeared leaving a dark brown liquid. The liquid, upon pumping over night, transformed to a bright solid which proved, from Raman spectroscopy, to be iridium pentafluoride.

2. The Cl_2/PtF_6 Studies

(a) The Stoichiometry of the Cl_2/PtF_6 Reaction

Typically, 100-200 mg of platinum hexafluoride was condensed into a quartz vessel held at -196°C , followed by an excess of chlorine. A slight blue color was observed on warming to -78°C . On warming further, a series of yellow, red-orange and red bands appeared along the wall of the reactor. As the temperature approached 23°C , a vigorous reaction took place. Excess chlorine was removed at -78°C , leaving a dirty yellow powder in the base with a further residue variegated from yellow to red on the wall. The vessel was held at room temperature with no apparent pressure increase. The nonhomogeneous nature of the solid implied the presence of at least two solid phases.

(b) Spectroscopic Studies of the Products of the Cl_2/PtF_6 Reaction

The reaction of chlorine and platinum hexafluoride was carried out in an identical manner to the analogous reaction of chlorine and iridium hexafluoride. Co-deposition of the two gases once again produced an intense blue solid on the Ag block/AgCl window cryo-tip. The infrared spectrum taken on the blue solid, shown in Figure IV-5, contains two new absorption bands, in addition to the ν_3 mode of

unreacted platinum hexafluoride. On one occasion, co-deposition of the two reactant gases produced a pale yellow solid product on the cold-surface. Its infrared spectrum, shown in Figure IV-5, contained only one new band. The Raman frequencies, obtained on the intense blue Cl_1/PtF_6 product, are given in Table IV-2 and discussed under Results and Discussion. Several attempts to obtain a Raman spectrum of the dirty yellow solid prepared in a quartz reactor at 25° and at -78°C were unsuccessful. The solid also proved to be amorphous to X-rays.

(c) Reactions of the Cl_2/PtF_6 Product(s)

(i) Reaction with NO

Nitric oxide was allowed to enter the quartz reactor containing a sample of the Cl_2/PtF_6 product at 23°C . No reaction was apparent at this temperature. On warming to approximately 50°C , the dirty yellow solid immediately took on a lighter yellow complexion. The volatiles above the solid consisted of NO and NOCl. An X-ray powder photograph of the solid residue showed the only identifiable diffraction pattern as that of $(\text{NO}^+)_2\text{PtF}_6^-$.^{13,18}

(ii) Reaction with Br_2

Bromine was first degassed at -80°C and distilled onto the dirty yellow Cl_2/PtF_6 reaction product at -196°C . The system was allowed to warm to 23°C with an apparent darkening after several minutes. The vessel was surrounded by boiling water (100°C) and a further darkening of the sample occurred. The resultant solid, now an almost red-brown color, proved amorphous to X-rays.

3. Spectroscopic Studies of the Cl_2OsF_6 Reaction

Co-depositing chlorine and osmium hexafluoride onto the 10°K

surface again produced a deep blue species. The infrared spectrum showed only one new band, centered at 540 cm^{-1} . The absence of a band in the $600\text{-}650\text{ cm}^{-1}$ region, where ν_3 of OsF_6^- occurs, indicated the inability of osmium hexafluoride to oxidize chlorine (at least to any significant extent).

Subsequently, excess chlorine was condensed onto osmium hexafluoride (200 mg) at -196°C . On warming to -78°C , a deep blue species was observed, which disappeared completely at 23°C . Recooling to $\sim -80^\circ\text{C}$ caused the blue species to reappear, but its color intensity had decreased considerably. Removal of chlorine at -78°C , following several warm/cool steps, left behind a yellow solid which proved to be pure osmium hexafluoride.

4. Spectroscopic Studies of the Cl_2/ReF_6 Reaction

The simultaneous deposition of chlorine and rhenium hexafluoride once again gave rise to the infrared absorption centered at 535 cm^{-1} . The blue species, however, did not appear, most likely due to the high concentration of rhenium hexafluoride. No absorption band attributable to ν_3 of ReF_6^- was observed--such a band would be expected in the $600\text{-}700\text{ cm}^{-1}$ region.

5. Spectroscopic Studies of the Cl_2/WF_6 Reaction

Excess chlorine was condensed at -196°C onto a sample of tungsten hexafluoride contained in the smaller type of quartz vessel described under II-A. No color change was observed in the mixture on warming toward 23°C . Removal of volatiles at -80°C left only tungsten hexafluoride.

6. Related Studies

(a) Reactions of $\text{Cl}_3^+\text{AsF}_6^-$

(i) C_6F_6

$\text{Cl}_3^+\text{AsF}_6^-$, prepared following the procedure of Gillespie and Morten,²⁰ was contained in a quartz reactor. WF_6 , followed by C_6F_6 , was distilled onto the sample at -196°C and the tube was warmed to 0°C using an ice bath. An immediate reaction took place with a pressure increase (Cl_2) to approximately 850 torr. Removal of excess C_6F_6 , WF_6 diluent and Cl_2 at 0°C left behind a small amount of finely divided yellow solid. Judging from the amount, some of the product presumably decomposed in the very exothermic reaction. Several attempts to obtain a Raman spectrum of this material at low temperature proved unsuccessful.

(ii) ONF

A small excess of ONF was condensed onto a sample of $\text{Cl}_3^+\text{AsF}_6^-$ contained in a quartz vessel at -196°C . The mixture was allowed to warm toward room temperature. When the pressure within the vessel reached approximately two atmospheres it was cooled again. This procedure was repeated several times to ensure complete reaction. An infrared spectrum of the volatiles taken following the reaction showed only ONF, NO_2 and ClF . The resultant white solid, from Raman spectroscopy, proved to be $\text{NO}^+\text{AsF}_6^-$.

(b) Reaction of $\text{Cl}_2\text{F}^+\text{AsF}_6^-$ with ONF

The reaction of $\text{Cl}_2\text{F}^+\text{AsF}_6^-$ (prepared as described by Christe and Sawodny²¹) with ONF was carried out in a similar manner as the $\text{Cl}_3^+\text{AsF}_6^-$ plus ONF reaction. The products, characterized using

Raman and infrared spectroscopy, were the same as in the previous reaction.

(c) Attempted Reaction of ClF with Ir₄F₂₀

A small quantity of Ir₄F₂₀ was placed in a teflon reaction vessel (made by heat-sealing one end of a 3/8 in. O.D. length of tubing and connecting the other end to a 1/4 in. Whitey valve via a 3/8 to 1/4 in. reducing union). Bromine pentafluoride was distilled onto the solid and the mixture was warmed to room temperature and agitated. An excess of ClF was then condensed into the vessel at -196°C. The tube was warmed toward room temperature until the pressure within the vessel reached approximately two atmospheres. It was then quenched with liquid N₂. This procedure was repeated several times. Some of the ClF was removed at -80°C until a pressure of two atmospheres was left in the vessel. The vessel was again carried through the cool/warm cycle; this time, however, it was warmed to room temperature. Removal of all volatiles at -22°C (liq. N₂/CCl₄) left a brownish-yellow solid which Raman spectroscopy proved to be the starting material Ir₄F₂₀.

C. Results and Discussion

All of the solid product spectra of the Cl₂/IrF₆ reaction can be resolved into three component spectra shown in Figure IV-4. Each of the spectra show a similar pattern of bands attributable to octahedrally coordinated atoms.

The Ir₄F₂₀ is the only structurally well-characterized product. The platinum metal pentafluorides have been shown from both single crystal^{22,23,24} and X-ray powder^{25,26} data to be isostructural. They

all consist of tetrameric units $(MF_5)_4$ with each metal atom octahedrally coordinated by F-atoms. The four octahedra are linked by single F-bridges. Each octahedron is involved in two such bridges in cis arrangement; i.e., each IrF_6 is highly distorted from regular O_h symmetry and has essentially C_{2v} site symmetry. Nevertheless, one recognizes that Ir_4F_{20} is a molecule built up from IrF_6 distorted octahedra. A stereoscopic view of $(RhF_5)_4$, which is the most precisely defined member of this group, is shown in Figure III-6.

The existence of Ir_4F_{20} in these systems implies that the $[IrF_5]$ monomer (see below) is unstable with respect to the F-bridged tetramer. Mutual F-ligand sharing provides the evidently desirable six coordination. One assumes that $[IrF_5]$ monomer would, given the opportunity, interact with like species to produce $[Ir_2F_{10}]$, $[Ir_3F_{15}]$ and finally Ir_4F_{20} .

Of course, interaction of $[IrF_5]$ monomer with fluoride ions immediately provides the octahedral IrF_6^- ion. Interaction of this with the monomer would produce the known $Ir_2F_{11}^-$ species.²⁷ It will be recognized, however, that in this latter species each IrF_5 entity derives less electron density from the contributed F^- ion than does the IrF_5 entity in forming IrF_6^- . On the other hand, the iridium atom in $Ir_2F_{11}^-$ is in a richer environment than the neutral compound Ir_4F_{20} . One can appreciate, therefore, that the electronegativity of the iridium atom increases from IrF_6^- to $Ir_2F_{11}^-$ to Ir_4F_{20} . The increasing electronegativity of the iridium atom in the series IrF_6^- to $Ir_2F_{11}^-$ to Ir_4F_{20} is presumably responsible for the general increase in frequency for the related sets of bands in the Raman spectra.

The initial identifiable product appears to be $\text{Cl}_3^+\text{IrF}_6^-$. The assignments of the anion frequencies can be made on the basis of other known salts containing the IrF_6^- ion; i.e., $\text{NO}^+\text{IrF}_6^-$, $\text{XeF}^+\text{IrF}_6^-$, $\text{ClO}_2^+\text{IrF}_6^-$ and $\text{ClF}_2^+\text{IrF}_6^-$.^{14,27} The Raman spectrum contains bands at 667, 555 and a doublet at ca. 215 and 238 cm^{-1} which can be assigned to ν_1 , ν_2 and ν_5 , respectively, of the IrF_6^- ion.

A pattern of Raman bands which increases in intensity with sample life is associated with a second product. These bands can be attributed to the $\text{Ir}_2\text{F}_{11}^-$ ion.²⁷ In the $\text{Ir}_2\text{F}_{11}^-$ ion, as with the well-characterized $\text{Sb}_2\text{F}_{11}^-$ ion,^{28,29} each metal atom is octahedrally coordinated by F-atoms with one F-atom in common. Bands appearing at 684, 566, 636 and a doublet at 216 and 262 cm^{-1} are attributed to the pseudo-octahedral modes " ν_1 ," " ν_2 ," " ν_3 " and " ν_5 ," respectively. Weaker bands appearing at 625 and 653 cm^{-1} are due to the octahedra in $\text{Ir}_2\text{F}_{11}^-$ being of lower symmetry than O_h ; moreover, the distorted octahedra are coupled by the bridging F-ligand.

The observation of the ν_3 mode in the Raman spectra of the two salts ($\text{Cl}_3^+\text{IrF}_6^-$, 624 cm^{-1} ; $\text{Cl}_3^+\text{Ir}_2\text{F}_{11}^-$, 636 cm^{-1}), as well as in the infrared spectra shown in Figures IV-2 and IV-3 (ca. 630 cm^{-1}) indicate that both anions are distorted from regular octahedral symmetry as a consequence of bridging to the cation.^{27,30} This departure from the mutual exclusion rule for molecules with a center of symmetry has been observed in a number of compounds containing octahedrally coordinated anions coupled to highly polarizing cations such as XeF^+ , ClO_2^+ , ClF_2^+ and Cl_2F^+ .^{27,14,20}

In both the $\text{Cl}_3^+\text{IrF}_6^-$ and $\text{Cl}_3^+\text{Ir}_2\text{F}_{11}^-$ salts, the Raman spectrum shows the same characteristic-stretching frequencies for the Cl_3^+

cation. Raman assignments of Gillespie and Morten²⁰ for Cl_3^+ are as follows: ν_1 , 490; ν_2 , 225; and ν_3 , 508 cm^{-1} and are based upon the vibrational frequencies of the isoelectronic SCl_2 molecule³¹ (514, 208 and 535 cm^{-1}). The same authors used the observed frequencies ν_2 and ν_5 with assumed values of the bond angle to calculate the stretching and bending force constants, 2.5 and 0.36 m dyne A^{-1} , respectively. The constants were then used to calculate the observed frequency ν_1 . A bond angle of 100° gave good agreement which compares closely with the observed bond angle of 103° for the SCl_2 molecule. The observed frequencies for Cl_3^+ in the iridium salt are almost the same as those for the arsenic salt. The values are compared in Table IV-3.

The final spectrum is that of the neutral compound Ir_4F_{20} . The strongest line in this spectrum at $\sim 720 \text{ cm}^{-1}$ can be attributed to a symmetric vibration related to the octahedral ν_1 mode. The band at 645 cm^{-1} is presumably the relative of $0_h \nu_2$ and the 200-300 cm^{-1} bands are the counterpart of $0_h \nu_5$. Weaker bands in the 650 to 710 cm^{-1} region cannot be simply related to octahedral modes.

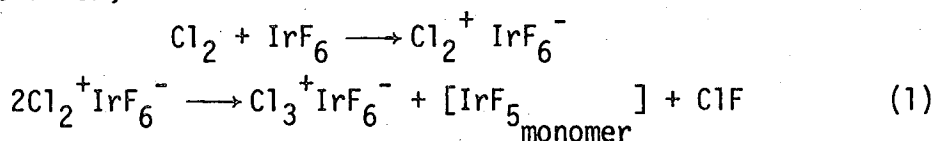
The Raman spectra of the initial product from the Cl_2 plus IrF_6 reaction at ca. 10°K (blue solid) and the product in the quartz reactor (pale yellow solid) are compared in Figure IV-1. The Cl_2^+ stretching frequency (645 cm^{-1}) is not observed in either of the spectra. It is possible that finely divided $\text{Cl}_2^+\text{IrF}_6^-$ would fail to provide observable Raman bands. Deposits of Xe/PtF_6 do not yield any Raman bands when the $\text{Xe}:\text{PtF}_6$ ratio is $\gg 1:1$ and only when $\text{XeF}^+\text{PtF}_6^-$ production becomes great enough (ratios $\ll 1:1$) is a band pattern (attributable to $\text{XeF}^+\text{PtF}_6^-$) observed.

Three new bands appearing in the Raman spectrum of the blue solid are absent from that due to the yellow solid. The first, appearing at 684 cm^{-1} is due to the ν_1 related mode of the $\text{Ir}_2\text{F}_{11}^-$ ion discussed earlier. The other two bands, appearing at 180 cm^{-1} (vs) and 355 cm^{-1} (broad) appear to be associated with the deep blue species. An infrared absorption centered at 540 cm^{-1} shown in Figure IV-2 is also associated with the blue color. The 540 cm^{-1} band is not far removed from the gas phase Raman shift of molecular chlorine (557 cm^{-1}). A similar infrared absorption (546 cm^{-1}) was observed by Clarke and Momantov³² on deposition of either neat chlorine or chlorine in inert matrices on an approximately 17°K cold surface at 3% or greater concentration. They argued that the peaks could only be attributed to molecular chlorine in an undefined weakly-bound complex. The observation of the blue color and the associated 540 cm^{-1} infrared band in the Cl_2/ReF_6 and the Cl_2/OsF_6 deposit and the absence of MF_6^- bands, indicate that the 540 cm^{-1} band is simply due to the Cl_2 stretch but presumably in some clusters which destroys the cylindrical Cl_2 symmetry and the most reasonable is a $\text{Cl}_2^+\text{MF}_6^-$ state or states. This charge transfer, however, cannot be extensive for the ReF_6 and OsF_6 cases, since the vibrational spectroscopy gives no evidence of MF_6^- . Recently Webb and Bernstein³³ showed from visible and UV absorption spectra that the opaque solution (purple in reflection) obtained by dissolving IrF_6 in liquid xenon is due to electron transfer from Xe to MF_6^- .

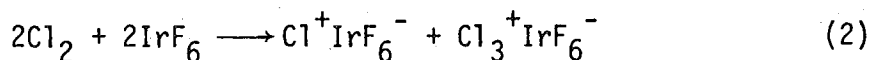
All other bands unaccounted for in the Raman spectrum of the blue solid arise from unreacted starting materials; (IrF_6 ; ν_1 699 cm^{-1} , ν_2 638 cm^{-1} , ν_5 260 cm^{-1})³¹ and (Cl_2 ; $\text{Cl}^{35}-\text{Cl}^{35}$ 535 cm^{-1} , $\text{Cl}^{35}-\text{Cl}^{37}$

527 cm^{-1} , $\text{Cl}^{37}\text{Cl}^{37}$ 520 cm^{-1}).

The gravimetric and tensimetric evidence indicate that initially chlorine had reacted with iridium hexafluoride in a mole ratio of approximately 1:1. The Raman and infrared data, however, indicate that the only chlorine-containing species associated with the IrF_6^- ion is Cl_3^+ . This might indicate that $\text{Cl}_2^+\text{IrF}_6^-$, produced initially, undergoes disproportionation,



but the failure to detect appropriate quantities of ClF in the products of the reaction allows for the possibility of the disproportionation



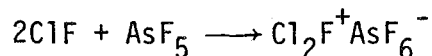
with this mixed oxidation state system perhaps being a double salt. The disproportionation represented by equation (2) does not appear to be energetically possible nor is the Cl^+ entity a species which one would expect to persist in an electron-rich environment (e.g., IrF_6^-) since Cl^+ is one electron pair short of the argon octet.

The first characterized salt containing the Cl_3^+ ion, $\text{Cl}_3^+\text{AsF}_6^-$, was prepared by displacement of ClF from ClClF^+ by Cl_2 to give the Cl_3^+ cation. Gillespie and Morton²⁰ recently suggested the Cl_3^+ cation as being derived from the interaction of Cl^+ with Cl_2 molecules.

A simple calculation of the heat of formation for the salt $\text{Cl}^+\text{IrF}_6^-$ based upon the electron affinity estimated by Webb and Bernstein³³ and the lattice energy given by Kapustinskii's equation³⁴ indicates that its enthalpy of formation is thermodynamically unfavorable by approximately 23 Kcal/mole. Even for the analogous Cl_2 plus PtF_6 reaction,

where the electron affinity is greater by about 25 Kcal, the calculated heat of formation is ca. zero. Thus since the entropy change in forming the salts is unfavorable, the likelihood of forming the Cl^+ ion in these systems is small.

In contrast to the above argument against the Cl^+ salts, the probability of producing the Cl_2^+ ion with both PtF_6^- and IrF_6^- anions is thermodynamically quite feasible. However, no thermodynamic barrier is anticipated for disproportionation to the more stable Cl_3^+ , $[\text{IrF}_5]$ and ClF species according to equation (1). However, since ClF and AsF_5 interact:



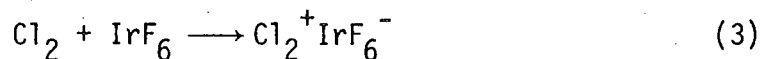
one anticipates that the generation of $[\text{IrF}_5]$ and ClF would result in $\text{Cl}_2\text{F}^+\text{IrF}_6^-$. There is no evidence, however, that this salt is produced in significant quantity in any of the reactions. Presumably the $[\text{IrF}_5]$ monomer plus Ir(V) anion reaction is favored over the formation of $\text{Cl}_2\text{F}^+\text{IrF}_6^-$. Furthermore, as cited earlier, the interaction of ClF with Ir_4F_{20} in BrF_5 solvent failed to produce the salt. It may be that $\text{Cl}_2\text{F}^+\text{IrF}_6^-$ and its relatives are thermodynamically unstable with respect to ClF and Ir_4F_{20} .

The molar susceptibility χ_m , versus absolute temperature T , plot for a sample of the Cl_2 plus IrF_6 reaction product is shown in Figure IV-7. The sample, prepared, as described in the Experimental section, was quickly transferred to the Dri-lab and loaded into the Kel-F sample capsule. It was then quickly cooled to liquid N_2 temperature. (The complete manipulation at room temperature took approximately 40-45

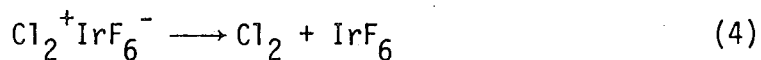
minutes.) The plot shows X_m to be essentially independent of temperature as expected for a quinquevalent iridium fluoro-complex. Therefore any cation must be diamagnetic.

The formation of the Cl_3^+ cation poses problems. To generate this species requires bond breakage in some Cl_2 species at some point in the synthesis. The bond energy of a neutral Cl_2 molecule is 58.2 Kcal/mole. It is not likely that free Cl atoms are ever produced.

As the gravimetric and tensimetric evidence show (see Table IV-1), the initial product has a stoicheometry at least close to $Cl_2:IrF_6$. It is reasonable on the basis of the known oxidizing capability of IrF_6 to assume that the first step is:



Since the vacuum transfer of this initial product always shows IrF_6 to be present in the volatiles, one can assume that (3) is reversible at ordinary temperatures. One can therefore assume that molecular Cl_2 can readily be available for conversion of Cl_2^+ to Cl_3^+ . Of course for each Cl_2 produced by the reverse charge transfer:

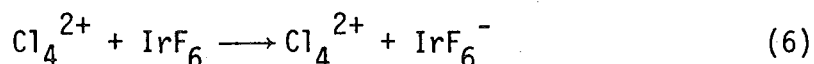


there will also be an IrF_6 molecule which is of course always able to act as an oxidizer. We can therefore visualize Cl_2^+ in an environment of Cl_2 molecules and IrF_6 molecules and IrF_6^- ions. Since Cl_2^+ possesses a half-filled π^* orbital in its ground state, it is possible that this ion (which has a high electron affinity) can act as a Lewis acid toward neutral Cl_2 .

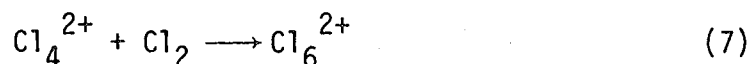


A species Cl_4^+ would involve very weak bonding between Cl_2 species. Thus a π type Lewis acid-base interaction of Cl_2 with Cl_2^+ would involve donation from the filled π^* m.o. of Cl_2 to the half-filled π^* m.o. of Cl_2^+ . The resultant bond between these molecules amounts to a one-electron bond.

The availability of IrF_6 to remove electrons means, however, that Cl_4^+ could be oxidized.

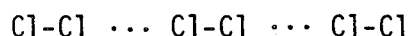


and Cl_2 neutral could add to Cl_4^{2+} in an analogous fashion to the initial Cl_4^+ generation:



The generation of the Cl_6^{2+} could, however, arise from Cl_6^+ , the latter coming from $\text{Cl}_4^+ + \text{Cl}_2$. In some such fashion Cl_6^{2+} could arise as the precursor to Cl_3^+ .

There are several geometries possible for Cl_6^{2+} and the electron rearrangement necessary to provide Cl_3^+ would probably be facilitated best by a chain:



Electron transfer from the terminal Cl_2 groups into the antibonding orbitals of the central Cl_2 would bring about the cleavage of that entity:

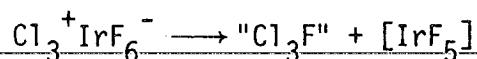


This accounts for the facile formation of the $\text{Cl}_3^+ \text{IrF}_6^-$ salt which is observed in the Raman spectra soon after the reaction and even at low temperatures.

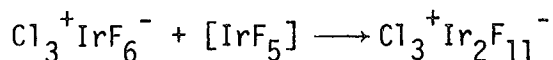
The bands appearing in the infrared spectrum at 10°K of neat Cl₂ (~ 546 cm⁻¹) are presumably due to Cl₂ in some sort of weakly-bound complex.³²

The low frequency bands appearing at 180 and 355 cm⁻¹ (possibly a harmonic) in the Raman spectrum shown in Figure IV-1(a) could be associated with the Lewis acid-base type one electron bonding in Cl₄⁺, Cl₆⁺ or even Cl₆²⁺-like species. At higher temperatures, (~ -80°C) the bands are absent, indicating complete transformation to Cl₃⁺. A similar pair of low-frequency bands were observed by Richardson¹⁴ when he reacted Cl₂ with the O₂⁺Sb₂F₁₁⁻ salt which were attributed to acid-base interaction of Cl₂ and O₂⁺.

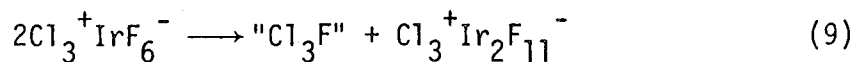
At room temperature the initial pale yellow solid, which vibrational data indicate is Cl₃⁺IrF₆⁻, transforms, over a two-day period, to the deep yellow-colored salt Cl₃⁺Ir₂F₁₁⁻. Presumably the reaction can be written simply as,



where some of the salt has decomposed into monomeric [IrF₅] and some unknown volatile species formulated here as "Cl₃F." The [IrF₅] monomer quickly reacts with an adjacent IrF₆⁻ ion



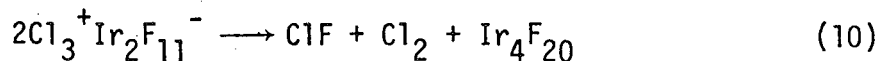
forming the Ir₂F₁₁⁻ ion. The net reaction is then



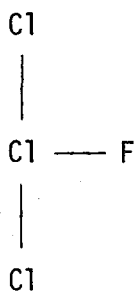
and it may well be a concerted reaction, as written.

In approximately one week at room temperature the initial solid had changed to a viscous liquid (see below) and in two or three weeks

finally produced a crystalline solid which proved to be Ir_4F_{20} .

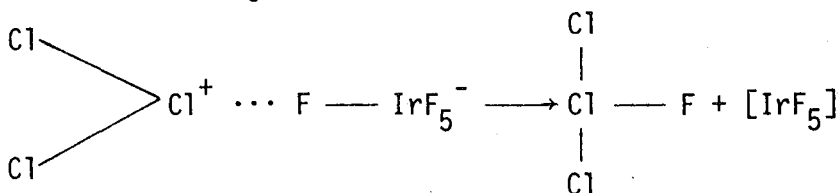


The gaseous species referred to as Cl_3F in reaction (9) gave an infrared absorption centered at 625 cm^{-1} (see Fig. IV-6). It has a half life of minutes only at room temperature, and thus far only small quantities have been isolated. Providing the Cl_3F formulation is correct, it would be analogous to BrF_3 or ClF_3 with C_{2v} site symmetry.

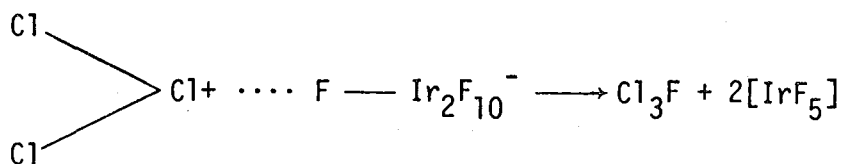


The PQR-type absorption centered at 625 cm^{-1} could be the ClF-stretching frequency for such a molecular configuration. Unfortunately the Cl-Cl absorptions would appear outside the range of the window (AgCl) frequency.

It is not difficult to visualize the formulation of Cl_3F by F^- ion abstraction from the IrF_6^- anion by the strongly polarizing Cl_3^+ cation.



The $[\text{IrF}_5]$ monomer would quickly react (perhaps in concerted fashion) with an adjacent IrF_6^- ion to yield $\text{Ir}_2\text{F}_{11}^-$. A second stage of the reaction could involve F^- abstraction from the $\text{Ir}_2\text{F}_{11}^-$ ion.



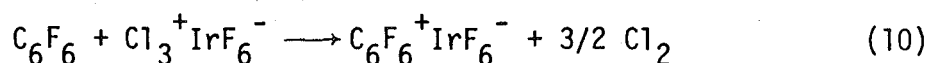
The monomeric $[\text{IrF}_5]$ could interact with like molecules producing the viscous liquid, $(\text{Ir}_x\text{F}_{5x})_{1 < x < 4}$, which slowly forms crystalline Ir_4F_{20} , the final product of (10). The thermally unstable Cl_3F decomposes into Cl_2 and ClF .

It should be noted that Cl_2F_2 radical was recently characterized by Mamantov and Andrews and their coworkers³⁵ by depositing premixed samples of $\text{Cl}_2/\text{F}_2/\text{Ar}$ onto a CsI cold window (10°K). The symmetric Cl_2F_2 molecule of C_{2v} site symmetry produced an absorption at $\sim 635 \text{ cm}^{-1}$ which was attributed to the antisymmetric stretch of the F-Cl-F unit. This molecule is expected to be more stable than Cl_3F , since the parent ion ClF_2^+ would carry a more localized positive center than Cl_3^+ . However, the parent ion ClF_2^+ was not observed in the reactions discussed here and therefore the likelihood of the absorption appearing at 625 cm^{-1} being due to Cl_2F_2 is small.

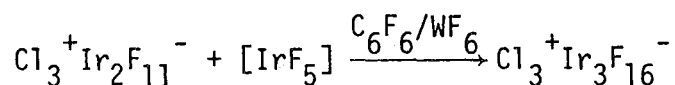
The reaction chemistry of the Cl_3^+ salts were investigated for two reasons: (1) to check the oxidizing capability of Cl_3^+ ion and (2) by using good fluoride ion donors, to attempt to displace the unknown volatile material formulated above as Cl_3F . Since Cl_2F_2 is a much more likely species than Cl_3F , the reaction of the $\text{Cl}_2\text{F}^+\text{AsF}_6^-$ salt was also investigated in an attempt to displace this material.

The initial product from the $\text{Cl}_2:\text{IrF}_6$ interactions reacts readily with C_6F_6 (I.P. = 9.97 eV) in WF_6 at approximately 0°C evolving Cl_2 gas. Removal of excess C_6F_6 , WF_6 and Cl_2 provided a yellow, free-flowing

solid similar to the solid formed from the reaction of C_6F_6 with IrF_6 in WF_6 .¹⁴ This solid was believed to be the $C_6F_6^+$ cation coupled to an Ir(V) anion, most likely IrF_6^- . The reaction can be written simply as



On the other hand, the reaction of C_6F_6 with the solid-liquid phase product (a mixture of $Cl_3^+ Ir_2F_{11}^-$ and its liquid decomposition product) in WF_6 solution showed no gas evolution. The Raman spectrum of the resultant orange-yellow solid shown in Figure IV-4 appears to be a mixture of $Cl_3^+ Ir_2F_{11}^-$ and $Cl_3^+ Ir_3F_{16}^-$. It is reasonable to suppose that the viscous liquid decomposition product, as mentioned above, consisted of some form of $(Ir_x F_{5x})_{1 < x < 4}$ which could be easily dissociated into monomeric $[IrF_5]$ in the presence of a suitable solvent. The monomeric $[IrF_5]$ would then quickly react with the $Ir_2F_{11}^-$ ion producing $Ir_3F_{16}^-$. Indeed, the C_6F_6/WF_6 mixture appears to have served only as a solvent. Presumably the reaction can be written as follows:



The $Ir_3F_{16}^-$ ion, prepared earlier by Bartlett and co-workers,²⁷ can be related to the analogous $Sb_3F_{16}^-$ ion reported by Edwards, James and Sills.⁷ Each metal atom is octahedrally coordinated by F-atoms with two of the F-atoms forming trans bridges at the central metal atom. The electronegativity of the iridium atoms in this configuration is less than in Ir_4F_{20} but greater than $Ir_2F_{11}^-$. An increase in frequencies for the species is therefore expected from IrF_6^- to $Ir_6F_{11}^-$ to $Ir_3F_{16}^-$ to Ir_4F_{10} . The Raman bands of $Ir_3F_{16}^-$ are in accord with these

expectations (see Figure IV-4) with the pseudo-octahedra ν_1 , mode (the most reliable assignment) appearing at 707 cm^{-1} . The assignments of the O_h related and " ν_2 ," " ν_3 " and " ν_5 " modes, given in Table IV-3, are at best tentative due to the impure nature of the sample. The variation in frequencies of " ν_1 ," " ν_2 " and " ν_3 " for IrF_6^- , $\text{Ir}_2\text{F}_{11}^-$, $\text{Ir}_3\text{F}_{16}^-$ and Ir_4F_{20} are given in Table IV-4.

The Raman frequencies observed for the Cl_2/PtF_6 reaction products at 10°C are given in Table IV-2. A broad band centered at 500 cm^{-1} can be related to the Cl_2/IrF_6 system, $\nu_3-\nu_1$ modes of Cl_3^+ . The two low-lying bands at 180 and 360 cm^{-1} may be the fundamental and first harmonic due to a vibration involving weak Lewis acid-base bonding in a complex of Cl_2 with Cl_2^+ . Other structural information is clearly desirable.

These findings are in harmony with the established increase in electron affinity of the third-series transition metal hexafluorides across the series from WF_6 to PtF_6 . Both PtF_6 and IrF_6 are clearly reduced in the $\text{Cl}_2 + \text{MF}_6$ reactions. Moreover, slight electron transfer evidently occurs with OsF_6 and even ReF_6 . Further investigations of these last systems by visible and UV absorption and near infrared spectroscopy are required to confirm this charge transfer.

TABLE IV-1. Tensimetric and gravimetric data for the $\text{Cl}_2 + \text{IrF}_6$ reaction.

Pressure (mm Hg) measured in a fixed volume					
Expt.	Initial IrF_6	Initial Cl_2	Residual Cl_2	$\text{Cl}_2:\text{IrF}_6$ Combining Ratio	Ref.
1.	77.0	185.5	130.5	1:1.4	*
2.	33.0	98.5	66.5	1:1.03	*
3.	180.0	380.0	165.0	1.19:1	**
4.	66.0	73.0	11.0	1:1.06	**
5.	123.0	125.0	0	1.02:1	**
6.	151.0	516.7	380.0	1;1.10	***
7.	165.0	320.0	120.0	1.21:1	***
8.	180.0	690.0	480.0	1.17:1	***
9.	295.0	865.0	520.0	1.17:1	***

Expt.	IrF_6	Cl_2/IrF_6 Adduct	Combined Cl_2	$\text{Cl}_2:\text{IrF}_6$ Mole Ratio	Ref.
1.	0.275g 0.898 m moles	0.339g -	0.064g 0.903 m moles	1.01:1	***
2.	0.595g 1.94 m moles	0.746 -	0.151g 2.13 m moles	1.10:1	***

*Ref. 13.

**S.P. Beaton, unpublished results.

***Present work.

TABLE IV-2. Raman bands for the $\text{Cl}_2 + \text{PtF}_6$ reaction product(s) at 10°K (blue solid).
(Frequencies given in cm^{-1} .)

704(s)	
680(s)	
646(w)	
628(w)	
$\sim 500(\text{s})$	---- $\nu_1, \nu_3 \text{Cl}_3^+$
360(s)	} Lewis acid-base type $\text{Cl}_2-\text{Cl}_2^+$ interaction modes
180(vs)	

TABLE IV-3. Raman spectra of known salts containing the Cl_3^+ cation. (Frequencies in cm^{-1} , relative intensities in parentheses.)

Compound	$\nu_1\text{Cl}_3^+$	$\nu_2\text{Cl}_3^+$	$\nu_3\text{Cl}_3^+$	Other Features
$\text{Cl}_3^+\text{AsF}_6^-$	493(100), 485(75)	225(75)	508(60)	<u>AsF_6^-</u> { $\nu_1 = 674(50)$ $\nu_4 = 394(6)$ $\nu_2 = 571(18)$ $\nu_5 = 370(25)$
* $\text{Cl}_3^+\text{IrF}_6^-$	490(89), 485(77)	225(20)	502(45)	<u>IrF_6^-</u> { $\nu_1 = 667(100)$ $\nu_3 = 624(20)$ $\nu_2 = 555(23)$ $\nu_5 = 238(66)$ 215(17)
* $\text{Cl}_3^+\text{Ir}_2\text{F}_{11}^-$	490(35), 485(32)	225(9)	502(26)	<u>$\text{Ir}_2\text{F}_4^{--}$</u> { " ν_1 " = 684(100) " ν_2 " = 566(15) 216(12) " ν_3 " = 636(18) " ν_5 " = 262(12)
* $\text{Cl}_3^+\text{Ir}_3\text{F}_{16}^-$	490(36), 485(?)	225(11)	502(22)	<u>$\text{Ir}_3\text{F}_{16}^{--}$</u> { " ν_1 " = 706(100) " ν_2 " = 570(11)*** " ν_3 " = 647(21) " ν_5 " = -

*This work.

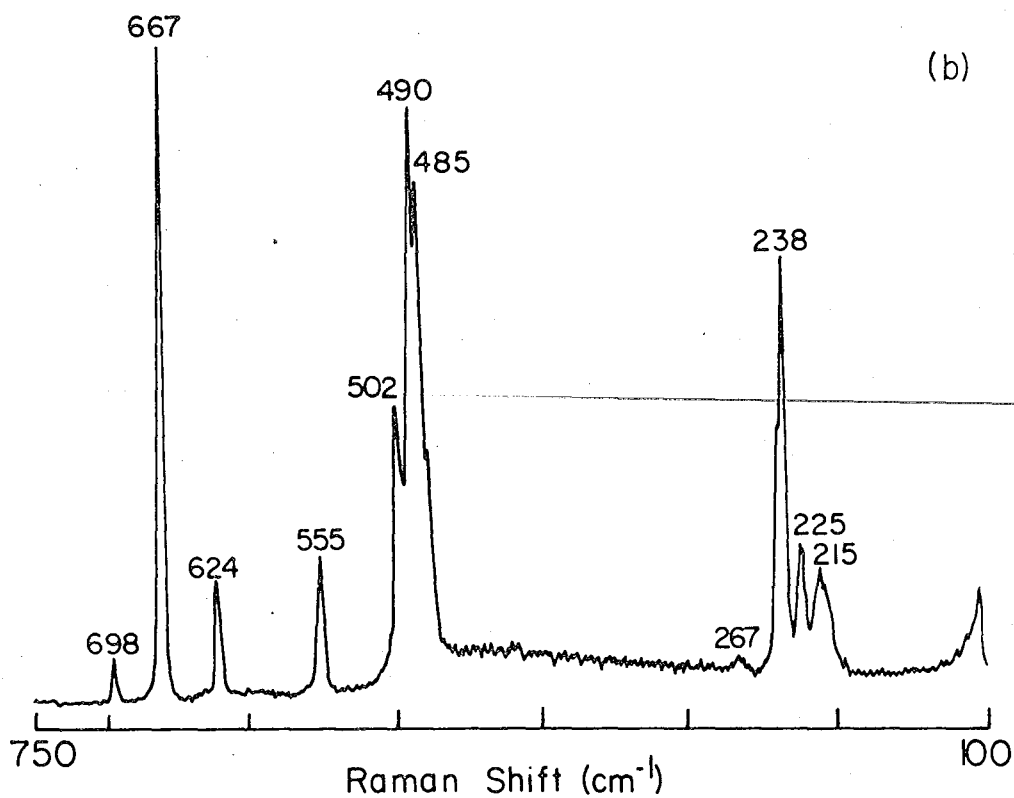
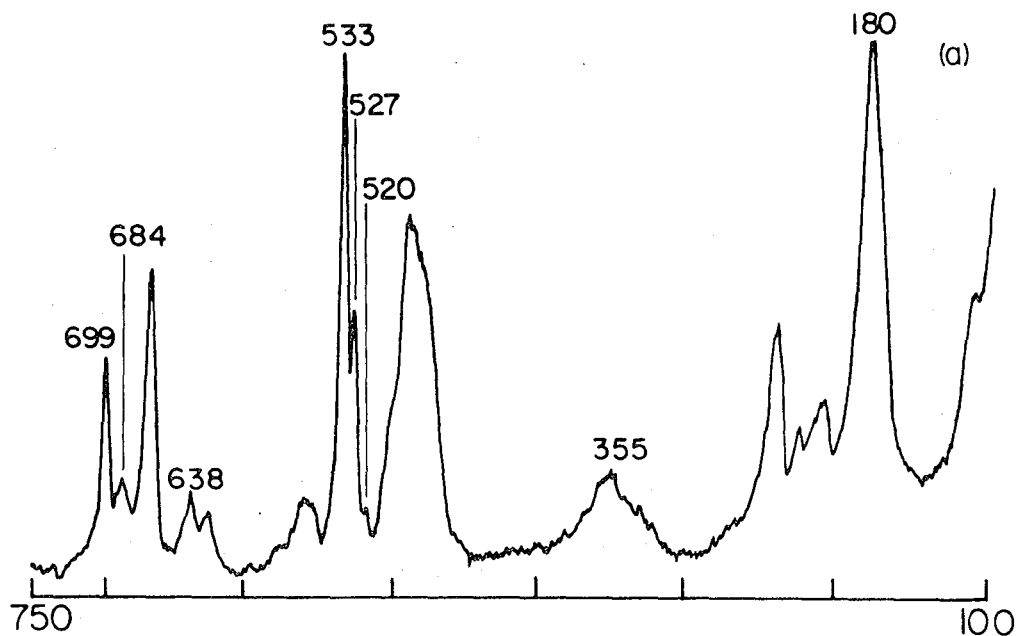
**The Ir atom is octahedrally coordinated in $\text{Ir}_2\text{F}_{11}^-$ and $\text{Ir}_3\text{F}_{16}^-$; therefore, octahedral mode descriptions are used although this is a crude description because of the non-equivalence of the F-ligands and must be very crude for $\text{Ir}_3\text{F}_{16}^-$ where one IrF_6 unit (the central one) is not equivalent to the other two.

***Uncertain assignment.

TABLE IV-4. Variation in frequencies of ν_1 , ν_2 and ν_3 for octahedrally coordinated Ir(V) species containing 0, 1, 2 and 4 bridging F-atoms.

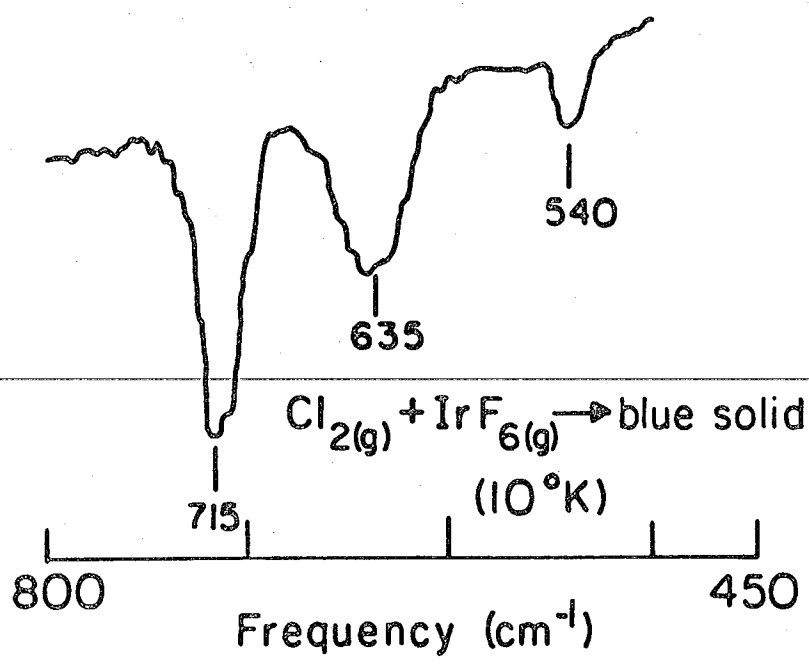
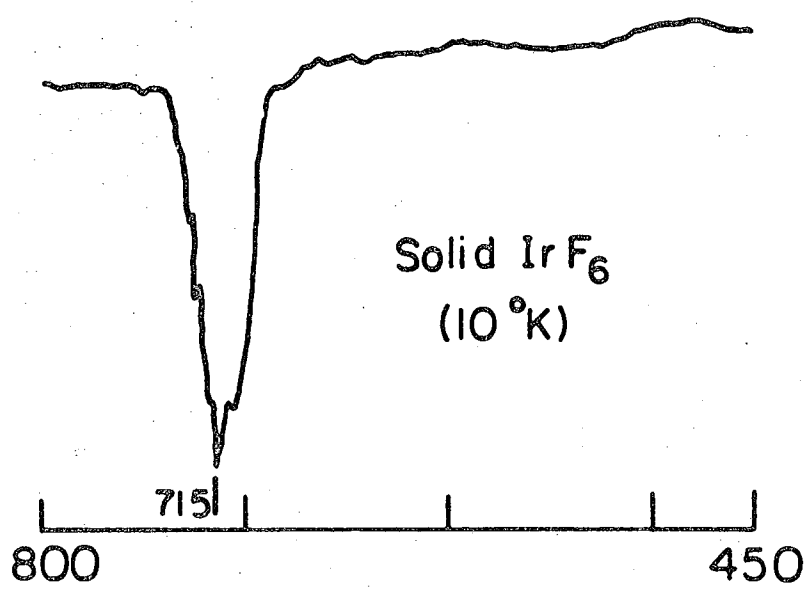
	Ir_4F_{20}	$\text{Ir}_3\text{F}_{16}^-$	$\text{Ir}_2\text{F}_{11}^-$	IrF_6^-
" ν_1 "	720	706	684	667
" ν_2 "	645	570*	566	555
" ν_3 "	-	647	636	624

*Uncertain assignment.



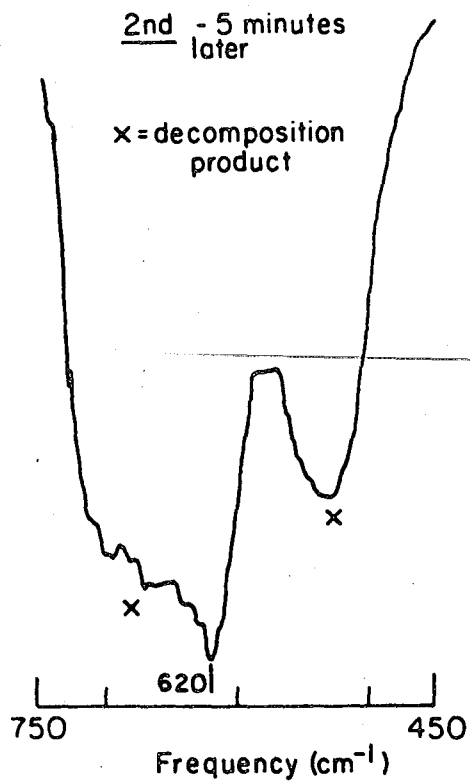
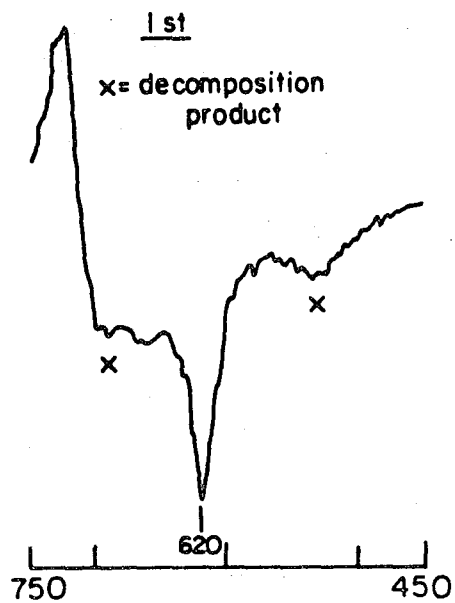
XBL 787- 5350

Figure IV-1. Raman spectra of $\text{Cl}_2 + \text{IrF}_6$ reaction products:
(a) blue solid at 10°K .
(b) pale yellow solid at -80°C .
(unnumbered bands in (a) are attributed to bands in (b)).



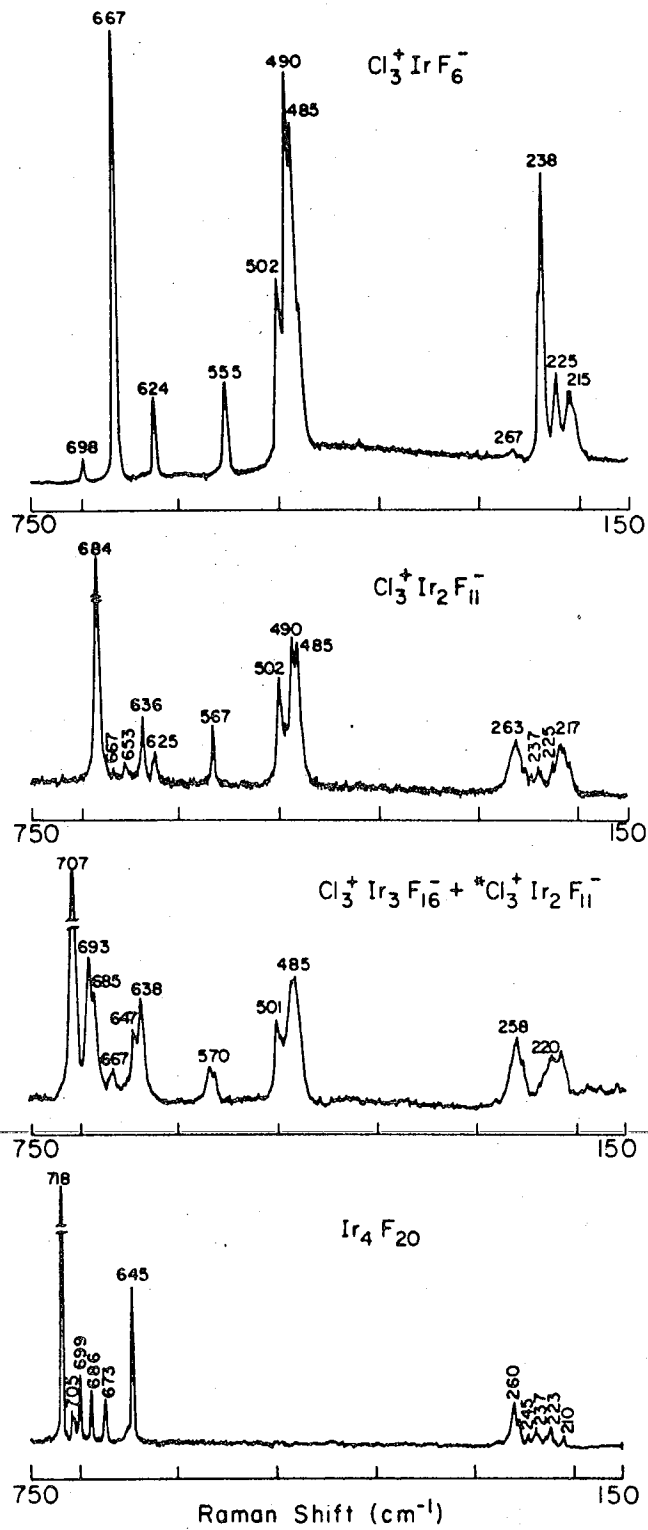
XBL 787-5351

Figure IV-2. Infrared spectra of $\text{IrF}_6(\text{s})$ and the initial Cl_2/IrF_6 reaction products.



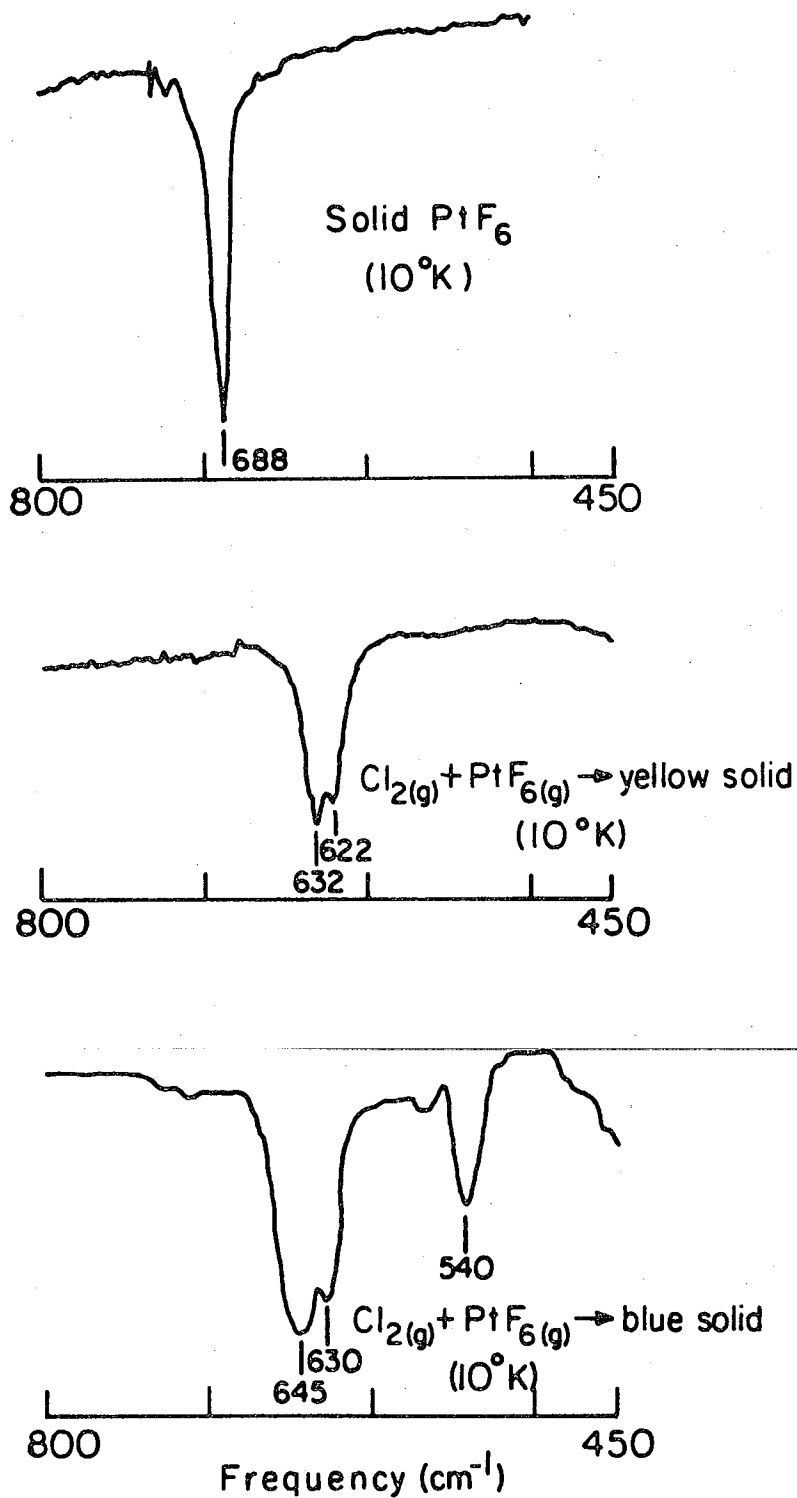
XBL 787-5353

Figure IV-3. Infrared spectra of room temperature Cl₂/IrF₆ product.



XBL 787-5349

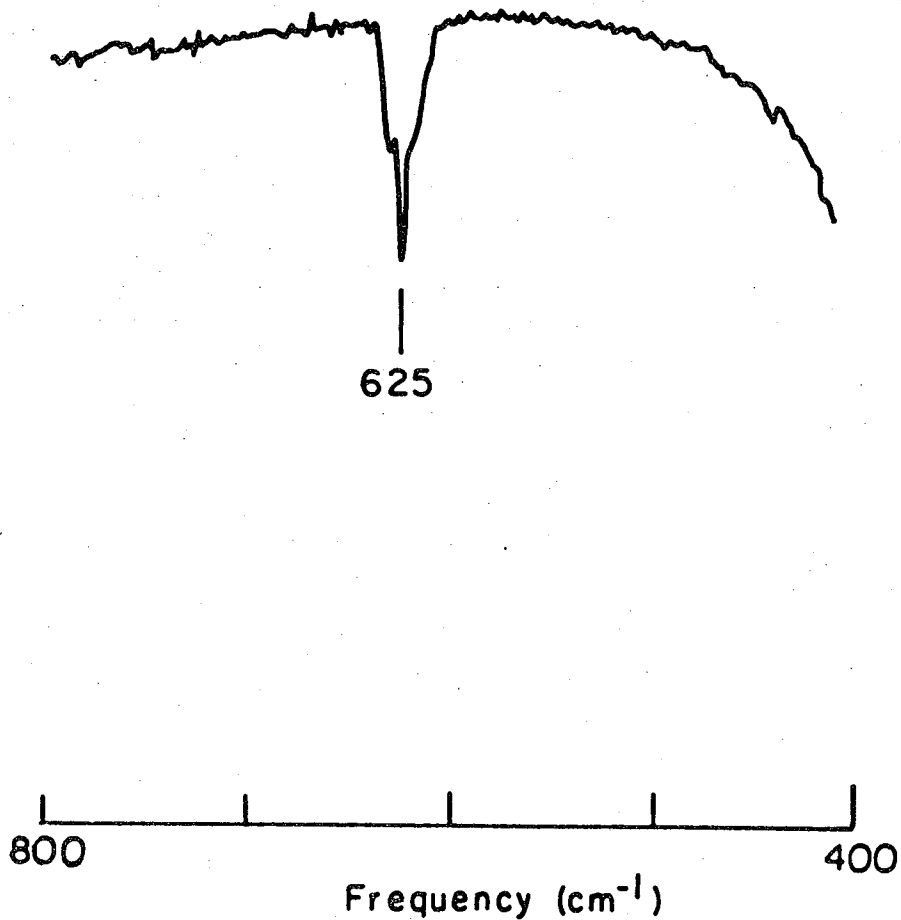
Figure IV-4. Raman spectra of $\text{Cl}_3^+ \text{IrF}_6^-$, $\text{Cl}_3^+ \text{Ir}_2\text{F}_{11}^-$, $\text{Cl}_3^+ \text{Ir}_3\text{F}_{16}^-$ and Ir_4F_{20} . Spectra taken at -80°C .



XBL 787-5352

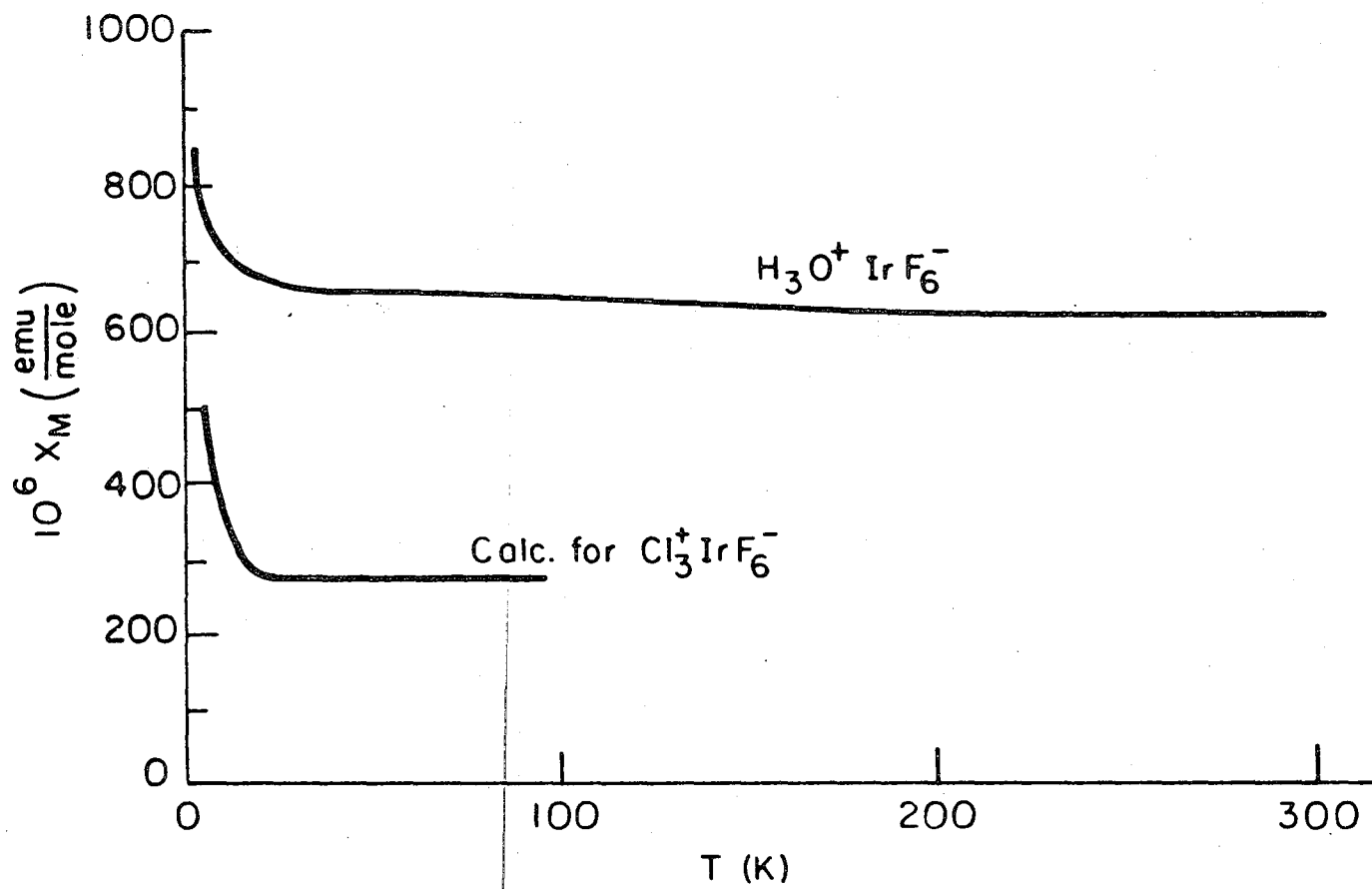
Figure IV-5. Infrared spectra of PtF_6 and the Cl_2/PtF_6 reaction products.

-86-



XBL 787-5354

Figure IV-6. Room temperature infrared spectrum of the volatiles from the room temperature decomposition of the Cl_2/IrF_6 solid product.



XBL 788-5678

Figure IV-7. $10^6 X_M$ vs. T plot for the Cl_2/IrF_6 reaction product and $*H_3O^+ IrF_6^-$.

*H. Selig, W.A. Sunder, F.A. DiSalvo and W.E. Falconer, J. Fluorine Chem. 11, 39 (1978).

REFERENCES

1. G. Herzberg, Molecular Spectra and Molecular Structure (Van Nostrand, Princeton, N.J., 1960) Vol. 1.
2. G.A. Olah and M.B. Comisarow, J. Amer. Chem. Soc. 90, 5033 (1968).
3. G.A. Olah and M.B. Comisarow, J. Amer. Chem. Soc. 91, 2172 (1969).
4. R.S. Eachus, T.P. Sleight and M.C.R. Symons, Nature 222, 769 (1969).
5. K.O. Christie and J.S. Muirhead, J. Amer. Chem. Soc. 91, 7777 (1969).
6. R.J. Gillespie and M.J. Morton, Inorg. Chem. 11, 591 (1972).
7. A.J. Edwards, G.R. Jones and R.J.C. Sills, Chem. Comm., 1527 (1968).
8. R.J. Gillespie and M.J. Morton, Chem. Comm., 1565 (1968).
9. R.J. Gillespie and J.B. Milne, Inorg. Chem. 5, 1577 (1966).
10. R.D.W. Kemmitt, M. Murray, V.M. McRae, R.D. Peacock and M.C.R. Symons, J. Chem. Soc., 862 (1968).
11. P.L. Robinson and G.J. Westland, J. Chem. Soc., 4481 (1956) and V.O. Ruff and J. Fischer, Z. Anorg. Chem. 179, 161 (1929).
12. N. Bartlett and P.R. Rao, Chem. Comm., 306 (1965).
- ~~13. N.K. Jha, Ph.D. Thesis, University of British Columbia, 1965.~~
14. T. Richardson, Ph.D. Thesis, University of California, Berkeley, 1974.
15. N. Bartlett, Angew. Chem. Int. Ed. 7, 433 (1968).
16. N. Bartlett and D.H. Lohmann, Proc. Chem. Soc. (London) 277 (1962).
17. N. Bartlett and D.H. Lohmann, J. Chem. Soc., 5253 (1962).
18. S.P. Beaton, Ph.D. Thesis, University of British Columbia, 1966.
19. M.A. Hepworth, P.L. Robinson and G.J. Westland, J. Chem. Soc. 4269 (1954).
20. R.J. Gillespie and M.J. Morton, Inorg. Chem. 9, 811 (1970).
21. K.O. Christie and W. Sawodny, Inorg. Chem. 8, 212 (1969).

22. B.K. Morrell, A. Zalkin, A. Tressand and N. Bartlett, *Inorg. Chem.* 12, 2640 (1973).
23. J.H. Holloway, R.D. Peacock and R.W.H. Small, *J. Chem. Soc.*, 644 (1964).
24. S.J. Mitchell and J.H. Holloway, *J. Chem. Soc. (A)* 2789 (1971).
25. J.H. Holloway, P.R. Rao and N. Bartlett, *Chem. Comm.*, 393 (1965).
26. N. Bartlett and P.R. Rao, *Chem. Comm.*, 252 (1965).
27. F.O. Sladky, P.A. Bulliner and N. Bartlett, *J. Chem. Soc.*, 2179 (1969).
28. V.M. McRae, R.D. Peacock and D.R. Russell, *Chem. Comm.*, 62 (1969).
29. A.J. Edwards and R.J.C. Sills, *J. Chem. Soc. (Dalton)* 1726 (1974).
30. M. Azeem, M. Brouwstein and R.J. Gillespie, *Can. J. Chem.* 47, 4159 (1969).
31. K. Nakamoto, *Infra-Red Spectra of Inorganic and Coordination Compounds*, 2nd Ed., p. 90.
32. M.R. Clarke and G. Mamantov, *Inorg. Nucl. Chem. Lett.* 7, 993 (1971).
33. J.D. Webb and E.R. Bernstein, *J. Amer. Chem. Soc.* 100, 483 (1978).
34. A.F. Kapustinskii, *Quart. Rev.* 10, 284 (1956).
35. E.S. Prochaska, L. Andrews, N.R. Smyrl and G. Mamantov, *Inorg. Chem.* 17, 970 (1978).

ACKNOWLEDGMENTS

I would particularly like to thank my research director, Professor Neil Bartlett, for his supervision and warm friendship throughout my graduate career. My association with this brilliant man will be forever cherished as a truly rewarding experience.

Thanks also to Dr. Norman Edelstein for assistance with magnetic susceptibility measurements, to Dr. Jim Scherer for use of the Raman spectrometer, and to Richard Biagioni for his aid in proof-reading this thesis.

Special thanks to Pamela Harris whose love, understanding and assistance prompted the completion of this work.

Finally, thanks to my parents, who taught me the meaning of patience.

This work was supported by the Division of Chemical Science, Office of Basic Energy Sciences, U.S. Department of Energy.

This report was done with support from the Department of Energy. Any conclusions or opinions expressed in this report represent solely those of the author(s) and not necessarily those of The Regents of the University of California, the Lawrence Berkeley Laboratory or the Department of Energy.

TECHNICAL INFORMATION DEPARTMENT
LAWRENCE BERKELEY LABORATORY
UNIVERSITY OF CALIFORNIA
BERKELEY, CALIFORNIA 94720